Thermodynamic Investigation of Human Nitric Oxide Synthase: Enzyme-Inhibitor Interactions

by

Zainab Hujee Al Hussain

A thesis
presented to the University of Waterloo
in fulfillment of the
thesis requirement for the degree of
Master of Science
in
Chemistry

Waterloo, Ontario, Canada, 2012

AUTHOR'S DECLARATION

I hereby declare that I am the sole author of this thesis. This is a true copy of the thesis, including any required final revisions, as accepted by my examiners.

I understand that my thesis may be made electronically available to the public.

Zainab Al Hussain

Abstract

Nitric oxide (NO) is produced in different mammalian tissues by nitric oxide synthase (NOS), which has three isoforms: neuronal NOS (nNOS), endothelial NOS (eNOS), and inducible NOS (iNOS). All NOS isoforms contain two domains, an oxygenase domain and a reductase domain. NO is an important transmitter of information between cells in many physiological processes; however, overproduction of this molecule may lead to health problems. Therefore, selective inhibition of NOS isoforms has useful therapeutic potential for treatment of certain diseases that can appear because of the pathological overproduction of nitric oxide. Producing useful isoform selective-inhibitors that bind to the active site in the oxygenase domain has proven to be difficult when based solely on the structure of these enzymes. Biophysical studies in combination with structural properties should provide better insights into isoform-specific inhibitor development. The first step of this study was to produce and purify truncated versions of NOS isozymes consisting of the oxygenase domain as they contain the active site of the enzyme. As a result of differences between humans and other mammals in the amino acids found in the second and third shells/layers surrounding the active site, all the experiments were performed with genes coding for human proteins. The major result of this project was the development of an Escherichia coli (*E. coli*) expression system to produce large amounts of pure protein. This system will allow for the testing of inhibitors that bind to the active site of NOS enzymes.

Acknowledgements

I would like firstly to express my thanks to ALLAH the Almighty for his grace, mercy and for the strength that I have been blessed with throughout my life.

A special thanks to my supervisor Dr. Guy Guillemette for all his amazing efforts in explaining the project in a simple and clear way. With his continuous tolerance and encouragement, he helped to make this thesis possible.

I would like also to thank my co-supervisor Dr. Monica Barra for her help, advice, and great ideas throughout my thesis-writing period.

I am grateful to my committee member Dr. Gary Dmitrienko for the time that he spent reading my thesis.

Many thanks too, to my colleagues and friends from the Department of Chemistry for their kind assistance and wise guidance to overcome some of the experimental problems.

I am greatly indebted to my beloved family and in laws for their encouragement in helping me to achieve success and reach my goal.

I'd like to express my heartfelt thanks and deepest appreciation to my husband, Youssef. Without his love, support and patience during the most challenging times I could not have completed my studies successfully. His reassurance throughout has been invaluable.

Finally I thank the Saudi Ministry of Higher Education, which provided me with all the financial support during my stay in Canada.

DEDICATION

To my husband, Youssef

And my kids, Nawaf and Ariana

Table of Contents

List of Figures

List of Tables

List of Abbreviations and Acronyms

Amp^r =Ampicillin resistance gene

δ-ALA = δ-Aminolevulinic acid

bp= Base Pair

CaM = Calmodulin

Cyt P450 = Cytochrome P450

DNA = Deoxyribonucleic acid

dNTP= Deoxynucleotide triphosphate

Δ*G* = Free energy change

Δ*H* = Enthalpy change

Δ*S* = Entropy change

ΔS_{solv} = Change in solvation entropy

ΔS_{conf} = Change in conformational entropy

ΔS_{mix} = Change in mixture entropy

***E. coli* =** Escherichia coli

eNOS = Endothelial NOS

FAD = Flavin-adenine dinucleotide

FMN = Flavin mononucleotide

GC= Guanylyl cyclase

H_4B = (6R)-5,6,7,8-tetrahydrobiopterin

Heme = Iron protoporphyrin IX

$hNOS_{oxy}$= Human nitric oxide synthase with oxygenase domain

ITC = Isothermal Titration Calorimetry

iNOS = Inducible NOS

IPTG= Isopropyl β-D-1-thiogalactopyranoside

IMAC= Immobilized metal ion affinity chromatography

K_a = Association equilibrium constant

K_d = Dissociation equilibrium constant

KDa= Kilodalton

Kan^r = Kanamycin resistance gene

L-Arg = L-Arginine

LB= Lysogeny broth

L-NMMA= L-N^G-monomethyl-L-arginine

L-NOHA= N$^\omega$-hydroxy-L-arginine

MQH$_2$O = Deionized water purified using a Milli-Q system (Millipore)

NADPH= Nicotinamide adenine dinucleotide phosphate

NHA= N-hydroxy-L-arginine

nNOS = Neuronal NOS

NOS = Nitric oxide synthase

OD$_{600}$= Optical density at 600 nm

PCR = Polymerase chain reaction

PET30a= Plasmid expression vector by T7 promoter

PFU= Pyrococcus furiosus

PWO= Pyrococcus woesei

P450= Pigment at 450 nm

RF= Restriction-free cloning

SDS-PAGE = Sodium dodecyl sulphate polyacrylamide gel electrophoresis

TB = Terrific broth

TCAG = The Centre for Applied Genomics

UV= Ultraviolet light

1400W = N-(3-(Aminomethyl)benzyl)acetamidine

Chapter 1
Introduction

1.1 Nitric Oxide

Nitric oxide has been the focus of intense study since its discovery. NO plays a major role in physiological processes such as neurotransmission, memory, blood pressure control, and the immune response. The molecular basis of NO action is to alter the activity of intracellular target enzymes rather than to bind to a receptor that regulates transcription (Ji *et al.*, 2009). Nitric oxide is a free radical compound (i.e., it has an unpaired electron) and is highly reactive (Vallance and Collier, 1994). *In vivo*, NO proliferates beyond cell walls but its effects are local within and between cells because NO is quite unstable and has a short half-life on only a few seconds (Kroncke *et al*., 1998). Even though nitric oxide is an extremely important regulator in many physiological processes in the mammalian body, it can also have negative impacts when it reacts with other reactive oxygen species (Huang *et al*., 2000).

1.2 Nitric Oxide Synthase Enzymes

The nitric oxide synthase (NOS, EC 1.14.13.39) enzymes catalyze the production of NO with L-citrulline through two successive mono-oxygenation reactions requiring reduced nicotinamide adenine dinucleotide phosphate (NADPH) and molecular oxygen (Alderton *et al.*, 2001) (Figure 1.1). These dimeric enzymes are composed of two monomers that contain both an oxygenase and a reductase domain. L-Arginine is first converted by a mono-oxygenase reaction to the intermediate N^{ω}-hydroxy-L-arginine (L-NOHA). This reaction involves oxygen insertion into the substrate and electrons originating from NADPH transferred to the reductase domain of the NOS

enzyme. The transferred electrons are shuttled from a flavin-adenine dinucleotide (FAD) to a flavin mononucleotide (FMN) in the reductase of one monomer and then to the heme iron in the oxygenase domain of a separate monomer. Upon arrival of the electrons at the oxygenase domain, there they interact with the heme iron (reducing Fe^{3+} to Fe^{2+}) and H_4B, allow it to activating the dioxygen bond. The second step of the NO synthesis reaction again involves the activation of a dioxygen molecule (Sabat *et al.*, 2009; Daff, 2010). In the second mono-oxygenase reaction, L-NOHA is oxidized to NO and L-citrulline.

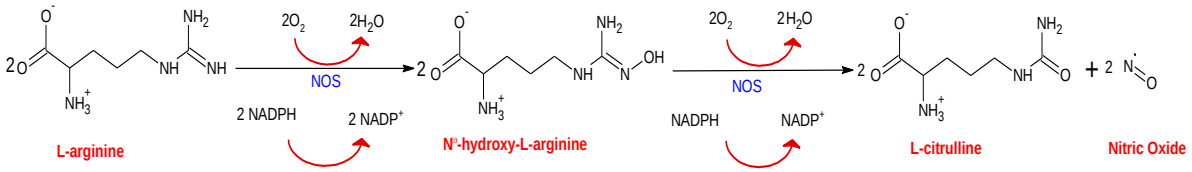

Figure 1.1: NOS catalyzed conversion of L-Arg to L-citrulline and nitric oxide, through intermediate N^{ω}-Hydroxy-L-Arginine. This reaction occurs in the presence of molecular oxygen and NADPH as the electron donor for each of the mono-oxygenase steps. This figure is derived from (Sabat *et al.*, 2009).

1.3 Characteristics of NOS Isoforms

NO is produced in different mammalian tissues by three known NOS isoforms: neuronal NOS (nNOS or NOS1), involved in neuronal signal transmission; endothelial NOS (eNOS or NOS3), involved in vascular endothelial cells; and inducible NOS (iNOS or NOS2), involved in the immune response. NOS isoforms are distinguished by their regulation and localization. For example, nNOS and eNOS are expressed constitutively in neurons and endothelial cells. However, NO is produced from these two isoforms as a signalling response, and these are

regulated by the intracellular concentration of Ca^{2+}−dependent Calmodulin (CaM) binding. In contrast, iNOS is Ca^{2+} −independent, and it is expressed in many tissue cells and requires an immunostimulant for its expression. This isoform produces nitric oxide as a product beneficial in host defense in the immune response, but also its expression produces nitric oxide as a cytotoxic agent in immune responses or inflammatory diseases (Haitao *et al.*, 2003; Stuehr, 1999).

The three isoforms of mammalian nitric oxide synthase have been extensively studied and characterized during the last 20 years. The three isoforms have a similar domain structure. As shown in Figure 1.2, each NOS subunit contains two domains: an amino-terminal oxygenase domain and a carboxy-terminal reductase domain. The two domains are linked by a calmodulin-binding motif. The NOS oxygenase domain contains the catalytic centre and binding sites for the substrates L-Arginine (L-Arg), molecular oxygen, catalytic heme, and the essential cofactor tetrahydrobiopterin (H_4B). Moreover, the oxygenase domains or the N-terminal regions of the NOS isoforms are different in length (Stuehr, 1999). The reductase domain contains binding sites for the cofactors flavin mononucleotide (FMN), flavin adenine dinucleotide (FAD), and NADPH. Calmodulin binding is required for the transfer of electrons from the reductase domain to the oxygenase domain (Igarashi *et al.*, 2009; Boyhan *et al.*, 1997). NOS is active in its dimer form with each monomer bound to L-arginine and five cofactors: FAD, FMN, heme, tetrahydrobiopterin (H_4B), and NADPH (Johnson, 2006). The oxygenase domain has the catalytic site for formation of NO.

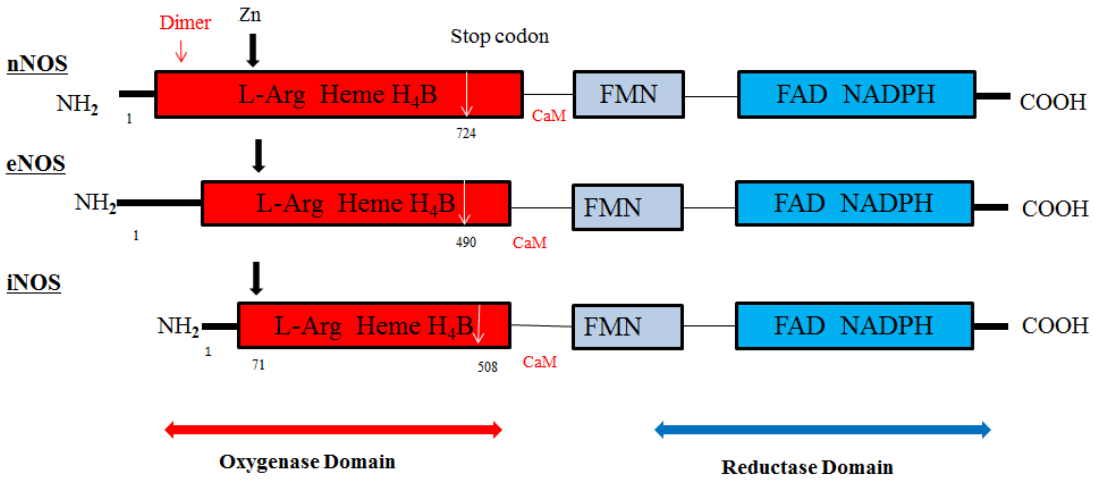

Figure 1.2: Domain structures of the three human NOS isoforms. This figure shows that all three isoforms share similar domain architecture. The numbers indicate the amino acid residue at the start and end of the oxygenase domain. The first arrow near the N-terminal indicates the dimer interface in the oxygenase domain, and the other arrow indicates the location of the stop codon. Figure 1.2 is derived from (Adrian *et al.*, 1999).

Crystal structures of the oxygenase domain of the three NOS isoforms have been analysed, and a number of X-ray crystal structures of dimers for iNOS, eNOS, and nNOS have been published (Alderton *et al.*, 2001). The crystal structure of the heme domain shows a zinc ion at the bottom of the dimer interface that coordinates to four cysteine residues, two from each monomer. The heme component is required for dimer formation. There are conflicting reports on the role of H_4B in the catalytic mechanism of NOS. It has been shown that the H_4B is a potential electron donor to the heme iron, which is required for oxygen activation. Moreover, crystal structures have shown that H_4B binds within the dimer interface and helps to stabilize the quaternary structure of the active enzyme form, NOS (Figure 1.3) (Raman *et al.*, 1998; Rafferty *et al.*, 1999; Daff, 2010).

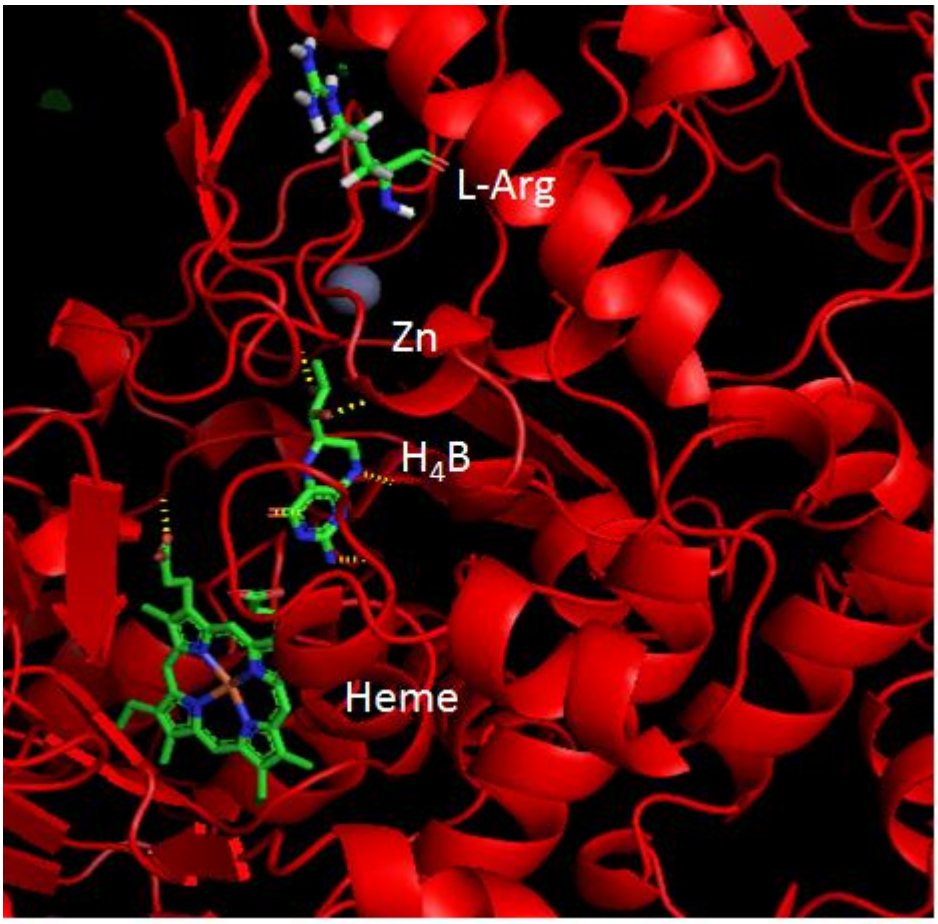

Figure 1.3: Active site (oxygenase domain) of Human nitric oxide synthase (PDB ID 4NOS).

The iNOS monomer is both catalytically inactive and cannot bind to either the substrate or the cofactor, H_4B (Crane *et al.*, 1997). The dimer form can bind substrates and H_4B and so is of some physiological importance (Crane *et al.*, 1998). Therefore, a dimer form of the oxygenase domain is required in this project for clarification of enzymatic activities and drug-ligand interactions (Figure 1.4).

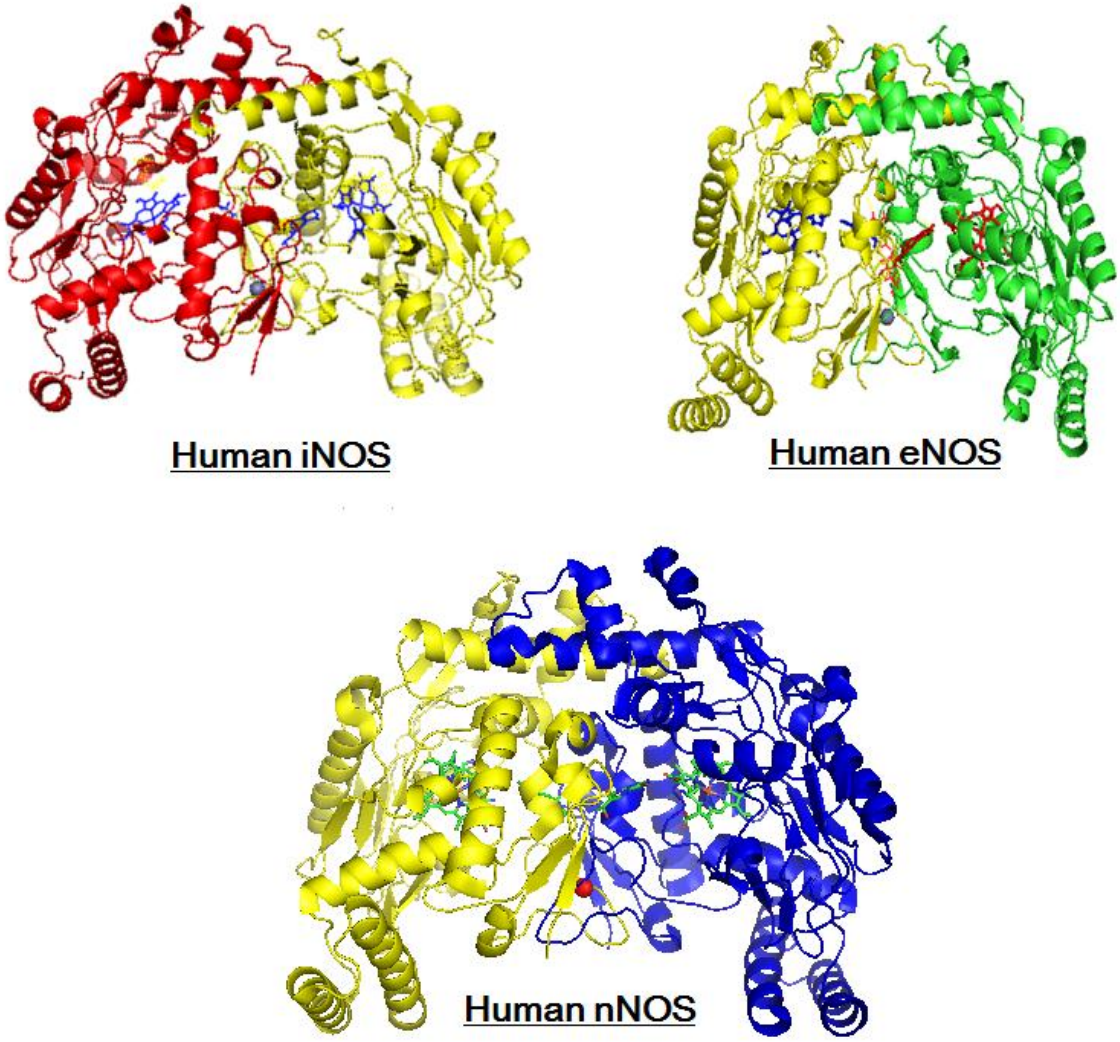

Figure 1.4: Dimer structures of Human iNOS (PDB ID 1NSI), Human nNOS (PDB ID 3DQR), and Human eNOS (PDB ID 3NOS) shown as ribbon diagrams. The structures show heme, L-Arg, H_4B, and Zn, which plays a role in dimer stabilization (Li *et al.*, 2001; Matter *et al.*, 2005; Fischmann *et al.*, 1999). This figure was made using PyMOL program.

Cloning of the three NOS isoforms has revealed that they share about 51-57% of the primary sequence identity and have an identical overall structure (Igarashi *et al.*, 2009). In addition, the three dimer structures of the isoforms are very similar, about 81-93 % identical (Salerno, 2002).

Human eNOS and iNOS not only have the same tertiary and quaternary structure, but also a close similarity in the active site residues found in the oxygenase domain of the protein. This high degree of structural and substrate-binding site similarity among isoforms has made it very challenging to produce isoform-specific inhibitors. The human and murine nucleotide sequences are approximately 80% identical (Garcin *et al.,* 2008).

1.4 NOS and its Therapeutic Potential

Under normal conditions, NO mediates the regulation of physiological processes. In contrast, uncontrolled generation of NO can cause unwanted pathologies such as septic shock, arthritis, diabetes, and asthma (Huang *et al*., 2000; Knowles and Moncada, 1994). Isoform-specific inhibitors of NOS enzymes have considerable therapeutic potential to combat certain diseases arising from NO overproduction. Enormous research efforts are taking place in this area to gain control of NOS within the human body. A century ago, NO was used as a cardiovascular medicine and vasorelaxant (Bauer *et al*., 1995). Recently, the majority of drug design in nitric oxide has been focused on NOS inhibitors. One of the biggest challenges in NOS related drug design is the fact that the oxygenase domains of the three NOS isoforms have very similar active sites (Figure 1.4). Indeed, an inhibitor must be specific to avoid undesirable side effects that might appear from the non-selective inhibition of the other isoforms. A major condition is ensuring that the inhibitory action does not affect eNOS activity, which has an important function in controlling blood flow and pressure. Therefore, the ideal inhibitors should inhibit NO over production by nNOS or iNOS that would result in pathological conditions, but should not disrupt NO generation by eNOS (Weber and Salemme, 2003; Grover and Wang, 2000).

Unfortunately, finding suitable inhibitors of the NOS isoforms has proven difficult because of the similarity among the active sites of the three NOS isozymes. Until now, inhibitors selective for NOS have been rare, of limited use and are sometimes toxic (Garcin *et al.,* 2008). However, despite all the similarities between the three isoform, some subtle structural differences in the NOS isoforms do exist and can lead to isoform selectivity. From a chemical point of view, inhibitors can be divided into two categories: amino acid-based inhibitors and non-amino acid-based inhibitors. It is possible to selectively inhibit one isoform of NOS by a simple modification of the guanidino group of L-Arg, in which the geometry and the size of the side chain are extremely important for selectivity. The underlying ideas in the design of these compounds are to increase selectivity and to better understand the preferred binding orientation of amino acid-based inhibitors within the arginine binding site (Adrian et al., 1999; Salerno et al., 2002). In order to improve the selectivity, non-amino acid-based inhibitors of NOS have been studied and these groups include a continually growing list of compounds containing a carbamidine carbon bound to either N (guanidines), S (isothioureas) or another C (amidines) (Salerno et al., 2002; Fishlock *et al*., 2003). Figure 1.5 briefly summarizes the two categories of NOS inhibitors.

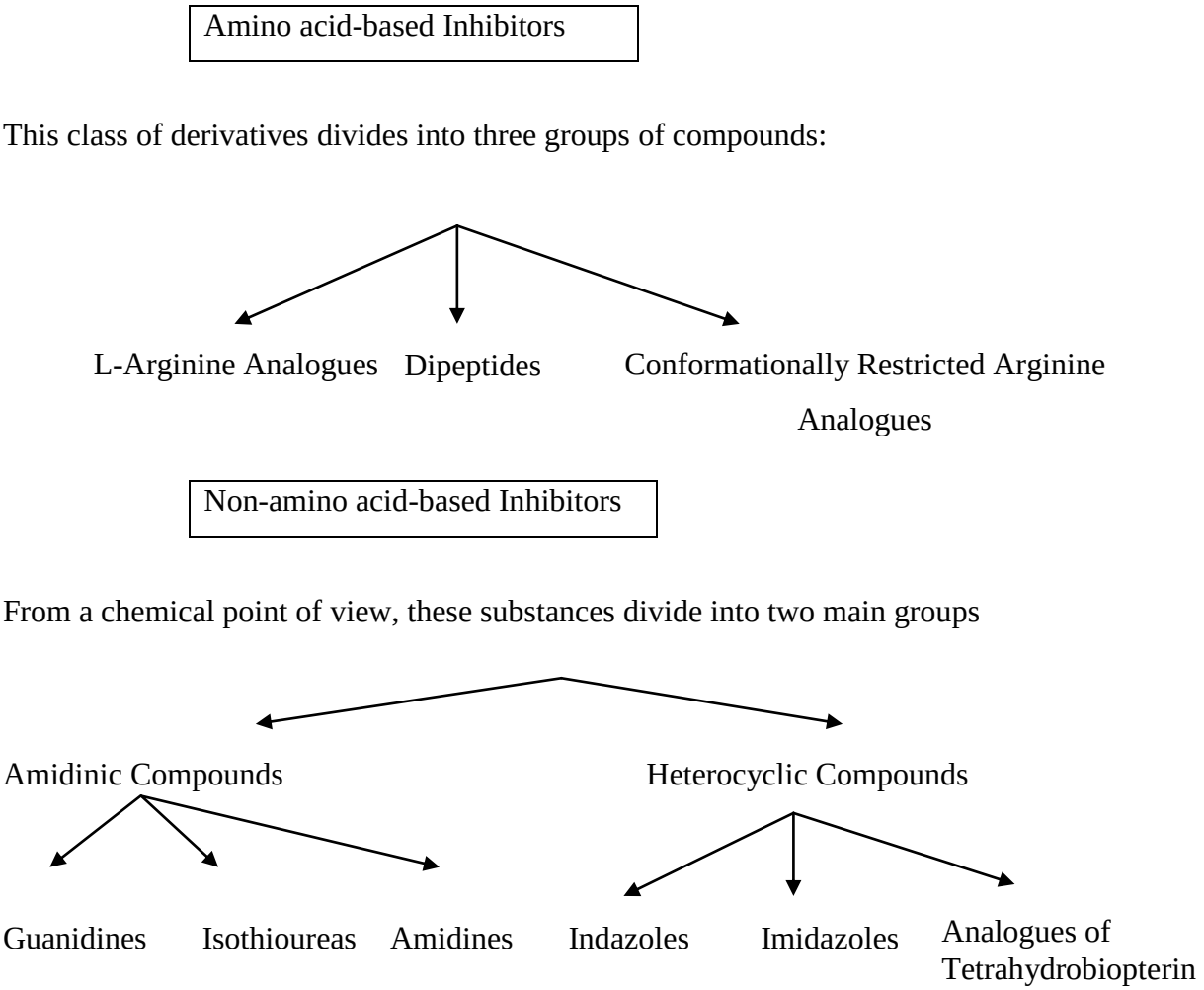

Figure 1.5: Classification of NOS inhibitors. This information is obtained from (Adrian et al., 1999; Salerno et al., 2002).

Numerous NOS inhibitors have been designed for therapeutic purposes; however, there has been little or no success in finding the perfect one. A good example of an isoform specific inhibitor from the non-aminoacid-based inhibitors group is N-(3-(aminomethyl)-benzyl)acetamidine (1400W), which was developed by Garvey *et al.,* (1994) (Figure 1.6). 1400W is a highly selective inhibitor for human iNOS versus both human eNOS and human nNOS. 1400W is

bound to the heme active site through hydrogen bonds to Glu 371, an amino acid residue responsible for the binding with guanidino group of L-Arg (Alderton et al., 2001). The selectivity of this inhibitor toward iNOS can be partly attributed to the higher turnover of iNOS compared to eNOS and nNOS, which leads to overproduction of peroxide and irreversible heme damage (Li *et al*., 2001). However, 1400W is acutely toxic at high doses; consequently, its use for therapeutic purposes is limited (Ji *et al*., 2009). As 1400W is readily available, it will be one of the initial inhibitors that will be used for the present investigation since it represents a good example of an isoform selective inhibitor.

Many attempts have been made to design isozyme-selective NOS inhibitors that target the active site in the oxygenase domain and can act as selective therapeutic agents but that do not have the potential for the side effects that may arise from inhibiting the other isoforms. Another thoroughly characterized NOS inhibitor, L-N^G-monomethyl-L-arginine (L-NMMA), will be included in our investigation. This compound is an example of an amino acid-based inhibitor and it is reasonably potent but not selective (Maddaford *et al*., 2009; Silverman, 2009). This inhibitor is commercially available, chemically stable, water soluble, and low in toxicity. Once adequate quantities of the oxygenase domains of the three NOS isoforms are available, both 1400W and L-NMMA will be used to test our theory that important information can be gained form biophysical studies performed on ligands that bind to the active sites of NOS isozymes.

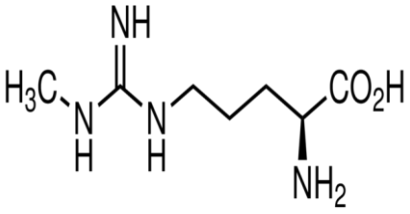

L-N^G-monomethyl-L-arginine (L-NMMA)

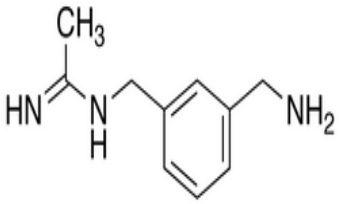

N-(3-(aminomethyl)-benzyl)acetamidine (1400W)

Figure 1.6: The structures of inhibitors of nitric oxide synthase.

1.5 Structure Based Inhibitor Design

The structure of the active sites of all three mammalian isoforms, iNOS, eNOS, and nNOS, are highly conserved. This is further complicated by the invariance in the composition of the active site residues that interact with L-arginine or the active site inhibitors. Figure 1.7 shows a simplified view of the active site, the residues that surround the active site and how differences in the outer shell residues may have a role in isoform specific binding. Simply put, the second shell residues interact with the first shell and the third shell residues interact with the second shell residues. There are apparent isoform specific differences in the residues found in the second and third layers/shells surrounding the first shell residues that form the active sites of the different NOS isozymes (Figure 1.7). In addition, differences exist in the second and third shell residues for the same isoform from different mammalian species. For example, there are slight differences between amino acid residues in humans and mice as shown in Figures 1.7 and 1.8. Therefore, an isoform-selective inhibitor that displays the desired pharmacological effects in mice may not do so in humans (Maddaford *et al*., 2009; Suh *et al*., 1998). This supports our approach of only working with the human versions of the NOS isozymes. There are also slight

differences in the second and third shell residues when comparing the three human isoforms of NOS as shown in Figure 1.8. Consequently, taking advantage of these differences may provide insight into the development of isoform selective inhibitors.

The anchored plasticity approach is a new method for designing such potent and selective NOS inhibitors (Garcin et al., 2008). For this approach, the crystal structures of the three NOS isoforms are used to identify an isozyme-specific induced-fit binding that is linked to a cascade of conformational changes that lie outside the active site. First, an inhibitor core is anchored in a conserved binding pocket, and then rigid tails oriented along pathways are extended to regions encompassed by second and third shell residues. This approach seeks to take advantage of the changes in flexibility and possibly residue composition away from the active site to optimize differences in isoform specific protein-inhibitor interactions. This method gives the general principles for the design of selective enzyme inhibitors that overcome strong active site conservation (Garcin et al., 2008; Maddaford *et al*., 2009).

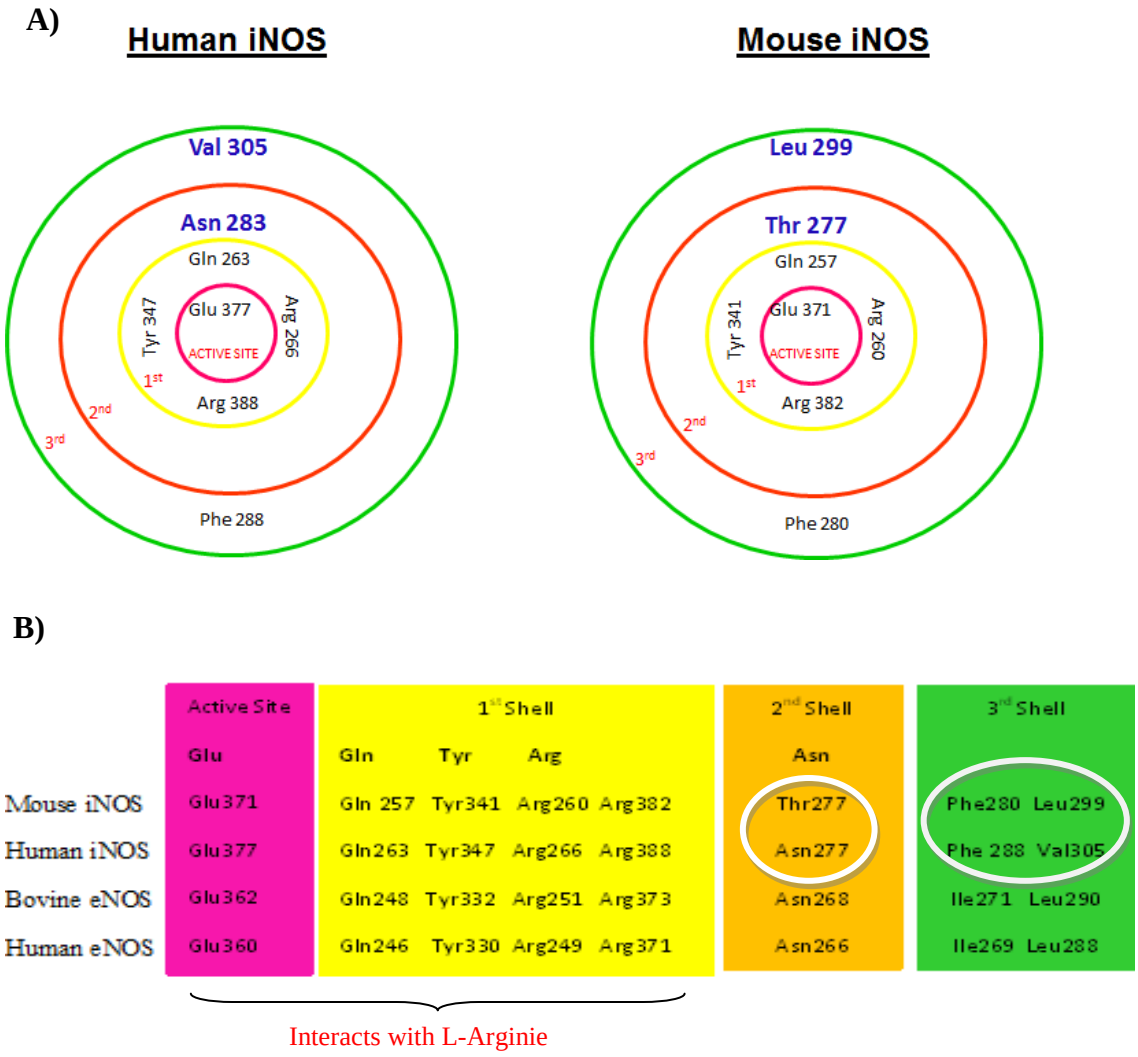

Figure 1.7: Amino acid residues for human iNOS and mouse iNOS involved in inhibitor binding. They are quite similar as indicated in this figure. The blue amino acids (A) and the two circles (B) indicate the slight differences between amino acid residues in active site residues (pink). The first-layer/shell (yellow) has almost similar residues making the selective creation of isoform- specific inhibitors difficult. In contrast, differences do exist between the isoforms in the second-layer /shell (orange) and third-layer/shell (green) residues that surround the active sites. Figure is derived from (Garcin *et al.*, 2008).

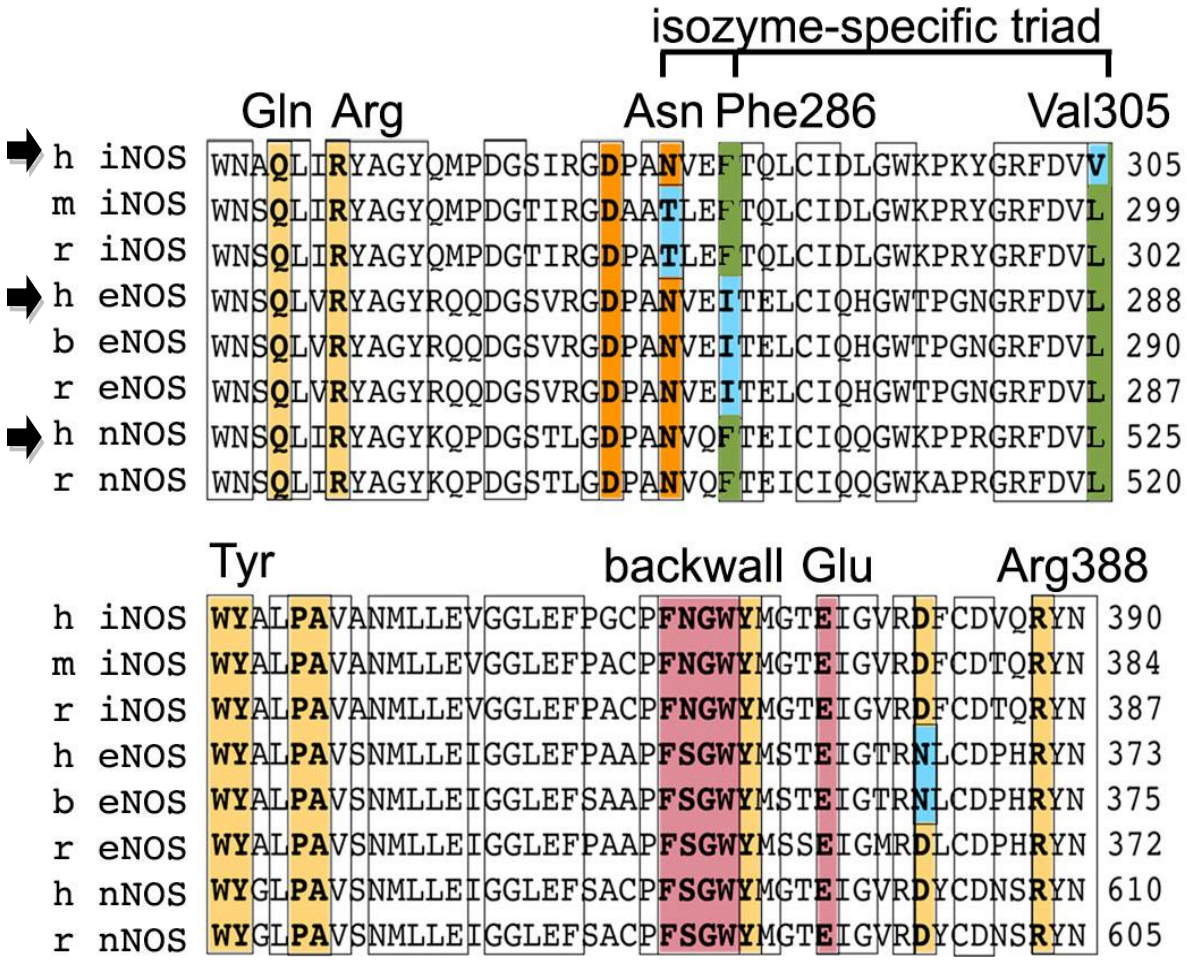

Figure 1.8: Amino acid sequence alignment for NOS isozymes. This figure shows the similarity between the three human NOS (hiNOS, heNOS, and hnNOS) as indicated by arrows. The residues are colored according to Figure 1.7. For all sequences, active site resides are shown in pink and include Glutamic (Glu), first-shell residues (yellow) include Glutamine (Gln), Arginine (Arg), and Tyrosine (Tyr), first shell is in contact with the inhibitor. Second-shell residues (orange) include Asparagine (Asn), and third-shell residues (green) include Phenylalanine (Phe) and Valine (Val). The slight differences among the residues are highlighted in blue. The key residues are indicated above the alignment and sequences are shown for human (h), mouse (m), rat (r), and bovine (b) NOS isozymes. Figure is derived from (Garcin *et al.*, 2008).

1.6 Biophysical Studies

Since NO's discovery in biological processes in the late 1980s, extensive efforts have been made to develop selective inhibitors based solely on structural knowledge, but these efforts have only rarely been successful. Therefore, more-detailed information about substrate and inhibitor binding to active sites is needed. One technique that can provide further information about macromolecule-ligand interactions is Isothermal Titration Calorimetry (ITC). ITC is used as a powerful tool in drug discovery and development (Azevedo and Dias, 2008). ITC provides thermodynamic data that links structure with function and clarifies the relationship between them.

Ligand association with proteins usually involves changes in the intermolecular interaction of the system components, including any component that may be present, such as the protein, the ligand, and water (Weber and Salemme, 2003). As a result, the changes in the bonding interaction that occur upon ligand binding lead to changes in the reaction enthalpy and entropy as well, which in turn determine the free energy of ligand association. Currently, many molecular or drug design strategies concern the optimization of binding affinity (Leavitt and Freire, 2001).

Isothermal titration calorimetry has been used extensively to measure thermodynamic parameters of substrate (L-Arg) binding to the oxygenase domain of NOS. The enthalpy and entropy determination are important in the design of high-affinity ligands and may increase the ability of potential inhibitors. ITC is highly sensitive, and able to measure a change in heat as small as 0.1 µcal. Studies of binding reactions with ITC provide, in one single experiment, the direct

thermodynamic parameters of the molecular interaction, such as the association constant (K_a), reaction enthalpy change (ΔH), free energy change (ΔG), entropy change (ΔS), and the dissociation equilibrium constant (K_d) whose relationship is shown in Eq (1.1).

$$\Delta G = -RTIn\,K_a = RTIn\,K_d = \Delta H - T\Delta S \qquad (1.1)$$

The change in reaction enthalpy of an inhibitor binding to an enzyme indicates the changes in weak interactions, such as electrostatic interactions, hydrogen bonding, and dipole-dipole interactions. The entropy of reaction reflects changes in conformation (ΔS_{conf}) and solvation (ΔS_{solv}) that occur when two species combine (ΔS_{mix}). Thus, the reaction entropy change is usually divided into three components that are involved when the inhibitor binds to the enzyme, shown in Eq (1.2) (Zakariassen *et al.,* 2008).

$$\Delta S = \Delta S_{mix} + \Delta S_{solv} + \Delta S_{conf} \qquad (1.2)$$

Generating isoform-specific inhibitors that bind tightly to the active sites is difficult with only structural data; however, ITC can provide thermodynamic information that is complementary to the structure. Assessing protein-ligand interactions is extremely important for drug development, and ITC experiments can be used to evaluate ligand-binding affinity. When a ligand binds to a protein, heat is absorbed or released. The changes in heat capacity indicate the hydrophobic interactions involved in binding. Figure 1.9 shows typical ITC-data; each peak represents the heat variation, which is proportional to the amount of binding in response to the serial addition of the ligand (Azevedo and Dias, 2008).

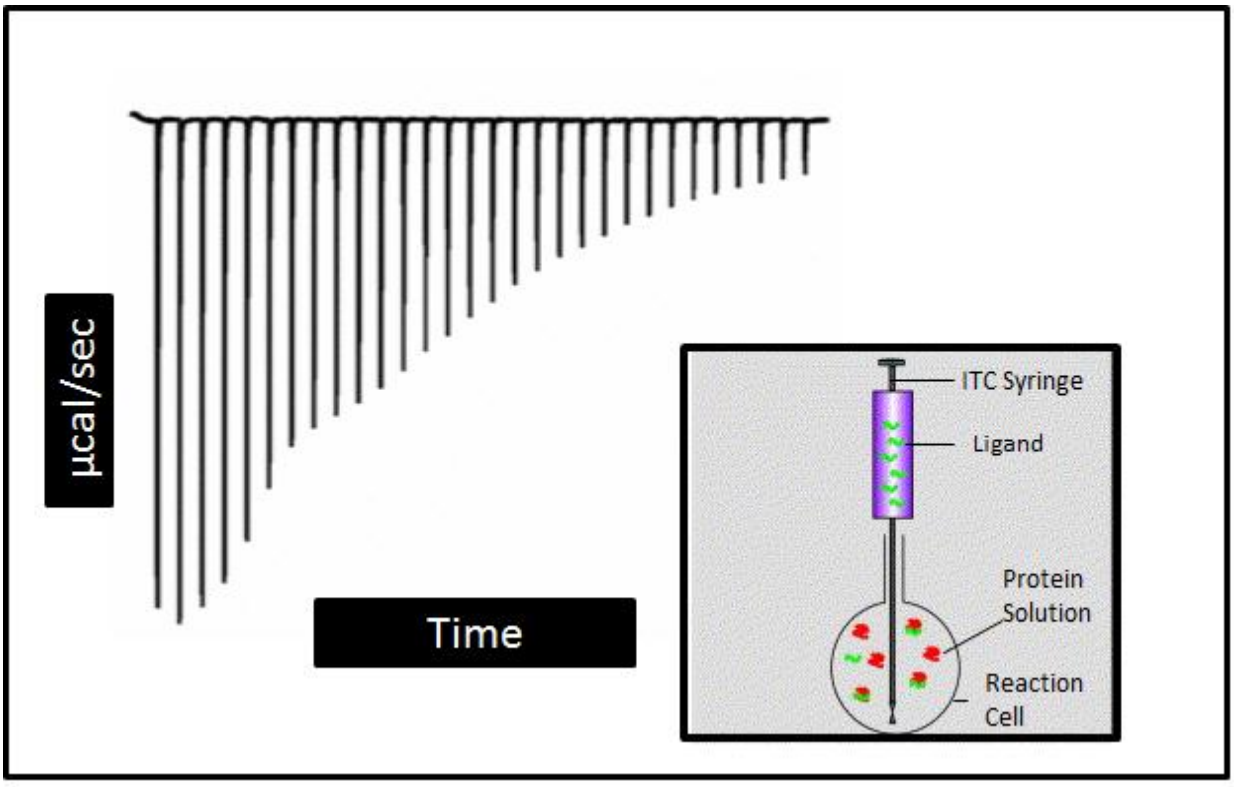

Figure 1.9: Typical Isothermal Titration Calorimetry (ITC) data. The inset illustrates the configuration of an ITC reaction cell. The reaction cell is filled with protein (red). The ITC injection syringe contains the ligand (green). Each peak in this figure presents the heat (microcalories) associated with this experiment. Figure is derived from (Azevedo and Dias, 2008; Leavitt and Freire, 2001).

An example of the use of ITC in the design of drugs is the case of cytochrome P450. Many studies have used ITC to predict enzyme-ligand interactions with mammalian P450 enzymes. The availability of such results could be a common feature of mammalian P450s defining the substrate selectivity and regio- and stereo specificities. ITC studies have been very useful in cytochrome P450 ligand binding studies. A similar approach is therefore valid for NOS as NOS and cytochrome P450 enzymes have similar properties.

1.7 Reason for studying Thermodynamic Ligand Binding of Human NOS Enzymes

Over the past years, research has been focused on clarifying the interactions between the NOS enzymes and inhibitors. Studying these interactions with their high bonding affinities is considered an important aim in drug development. A highly purified protein was needed for the investigation of the thermodynamic properties of ligand binding. The project started with molecular biology. The amplified target fragments were cloned into PET plasmids. These vectors contain several important elements (e.g., *lacI* and T7 promoter) for production of desired protein when activated. Moreover, the design of this system allowed easy overexpression of a desired protein and control of when that expression occurs. Then the biophysical characterization of the human NOS isoforms was done to double check purity, size, and to calculate the concentration of the desire proteins. Generation of recombinant expression and purification protocols facilitated the use of ITC as it requires highly purified protein.

1.8 Research Goals

The main goals of this research project were, first, to develop a system to express and purify the oxygenase domains of the three human NOS isoforms. Second, to perform biophysical studies to characterize the recombinant NOS isoforms. Finally, to use ITC to gain knowledge of the thermodynamic properties of inhibitors binding to the different NOS isoforms. A better understanding of the biophysical properties of ligand binding to the enzyme active sites may pave the way for the development of better isoform-specific inhibitors.

To achieve these goals, the following steps are required:

I. Develop expression systems for the oxygenase domains of human iNOS, human eNOS, and human nNOS isoforms, using a polymerase chain reaction (PCR), because the oxygenase domains contain the active site;

II. Optimize purification procedures for the oxygenase domains by combining metal chelation and gel filtration chromatography for purification and to verify dimer formation, and

III. Characterize the physical properties of the purified recombinant proteins.

Chapter 2
Generation of *Escherichia coli* Overexpression Systems for the Production of Human NOS Oxygenase Domains

2.1 Introduction

We proposed to study only the oxygenase domain of the human NOS enzymes and therefore required a recombinant expression system. This was accomplished by separating the oxygenase domains of NOS isoforms from the reductase domains because the oxygenase domain contains the enzyme active site (Figure 2.1). The NOS active site is responsible for the selective binding of L-Arginine and the active site inhibitors planned to be used in the future of this project. The desired coding regions were amplified using the polymerase chain reaction (PCR) with specifically designed oligouncleotide primers. The mutagenesis by PCR was used to increase gene expression through the modification of a specific codon. Two PCR strategies were involved in sub-cloning the oxygenase domains. The first was polymerase chain reaction sub-cloning for human iNOS (hiNOS), and the second was restriction-free (RF) cloning for human nNOS (hnNOS) and human eNOS (heNOS). For hiNOS the restriction enzymes were needed to obtain the wanted fragment and to ligate it into an expression vector. As the ligation experiment was time consuming and difficult, another technique was used for heNOS and hnNOS: the RF cloning. The concept of this experiment is to insert a deoxyribonucleic acid (DNA) fragment into circular plasmid with no need to use restriction sites, ligation, or alterations in either the vector or the gene of interest (Van den Ent and Lowe, 2006).

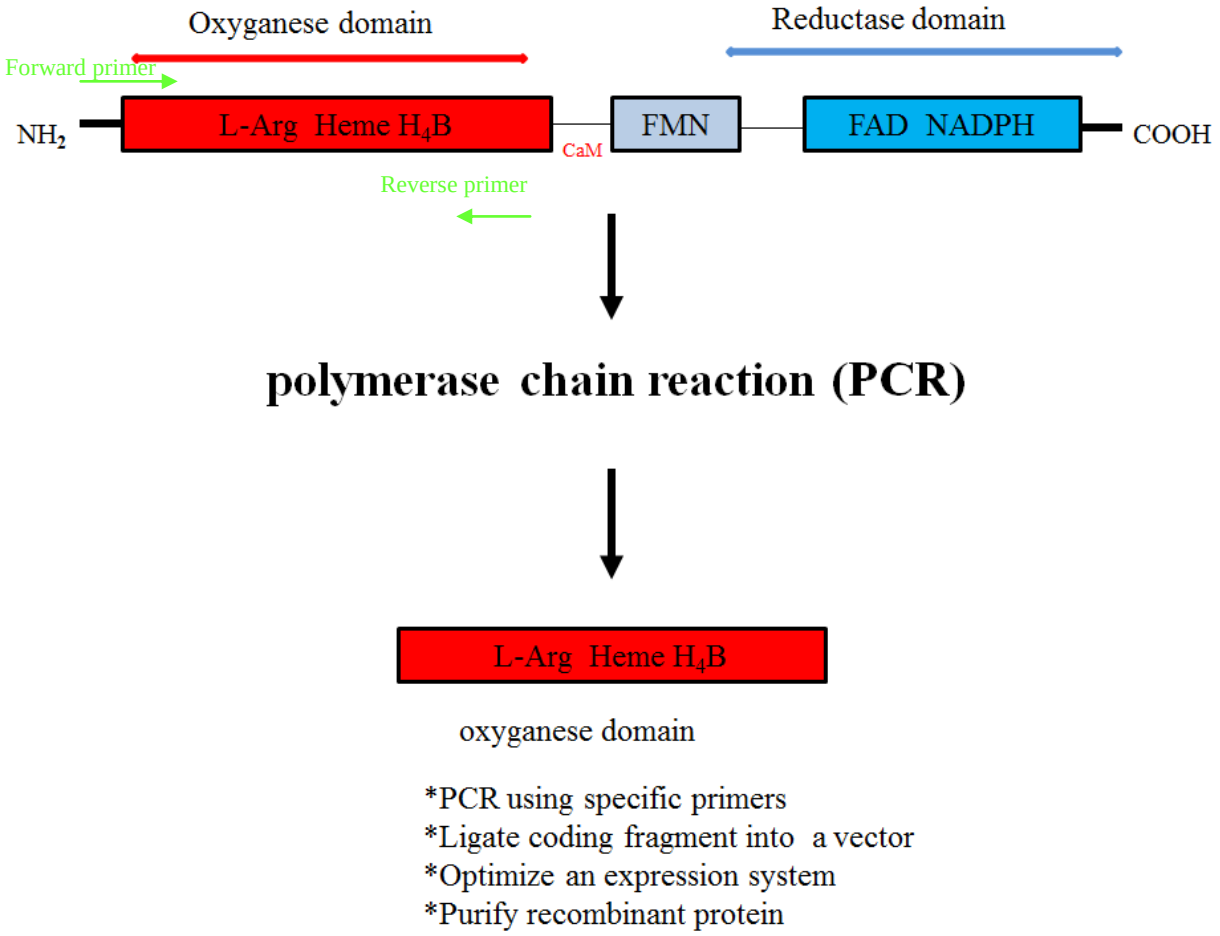

Figure 2.1: Separation of the human NOS domains with a brief outline of the steps involved in the expression system of NOS (Newton, 1997).

2.2 Experimental Techniques

2.2.1 PCR Mutagenesis of Human iNOS Isoforms

The human iNOS (delta70) in PcWori (8226bp) was used as template to insert into PET-30a (+) vector. The cloning of the human iNOS oxygenase was performed by amplifying the coding region for human iNOS expression vector supplied by Dr. Dipak Ghosh of Duke University. The

expression vector for the oxygenase domain for human iNOS had already been designed in our laboratory by Amanda Harrop, a fourth year student. It contains a Hind III stop codon in the pcWori vector. Human iNOS was cloned using a PCR to create a linear DNA fragment. In PCR, as a general condition, the temperature went through three stages: denaturation at 94-96 ºC, annealing at 65 ºC, and elongation at 72 ºC. In many cases, a hot start is an important step in improving the specificity of PCR. The mutagenesis for hiNOS was done using a Pyrococcus furiosus (PFU) polymerase kit (Fermentas Molecular Biology Tools), a 10x PFU buffer with $MgSO_4$, an hiNOS template, MQH_2O, deoxynucleotide triphosphate (dNTP), a forward primer, and a reverse primer (Figure 2.2). The template DNA was human iNOS delta 70 in pcWori vector. The primers were designed to amplify the desired region of the hiNOS and to introduce restriction endonuclease recognition sites for both Hind III and a polyhistidine tag to help later on in the purification process. The PCR products were then run on an agarose gel, and the desired fragment of intact DNA was isolated from the agarose gel using the protocol as per the "QLAquick Gel Extraction Kit Protocol using a microcentrifuge" (QIAGEN). The desired product was verified by sequencing.

After inserting the stop codon into the PcWori, two techniques were applied. First, the vector was digested with HindIII and then it was allowed to self-ligate (self-circulated). Second, the vector was digested with HindIII and NdeI and transformed it from PcWori vector to PET vector was digested with the same restriction enzymes, HindIII and NdeI, (Figure 2.3).

hiNOS FOR

5' CGCAATGCCCCTCGAGCCATTGGGAGAATCCAGTGGTCCAAC 3'

hiNOS REV

5' GTTGGACCACTGGATTCTCCCAATGGCTCGAGGGGCATTGCG 3'

heNOS FOR

5' CACCATCATCATCATCATTCTTCTGGTATGGGCAACTTGAAGAG 3'

heNOS REV

5' TTGTCGACGGAGCTCGAATTCGGATCATTAGATGCCGGTGCCC 3'

hnNOS FOR

5' CACCATCATCATCATCATTCTTCTGGTATGGAGGATCACATGTT 3'

hnNOS REV

5' TTGTCGACGGAGCTCGAATTCGGATCATTAGGTGCCTTTCCAG 3'

Figure 2.2: Primers used for the amplification of human NOS. For hiNOS, two primers were used for sub-cloning the oxygenase domain from leucine (Leu)71-proline (Pro) 508. The heNOS primers were used to amplify the coding region from methionine (Met) 1-isoleucine (Ile) 490. The primers for hnNOS were used to amplify the coding region from methionine (Met) 1-threonine (Thr) 724.

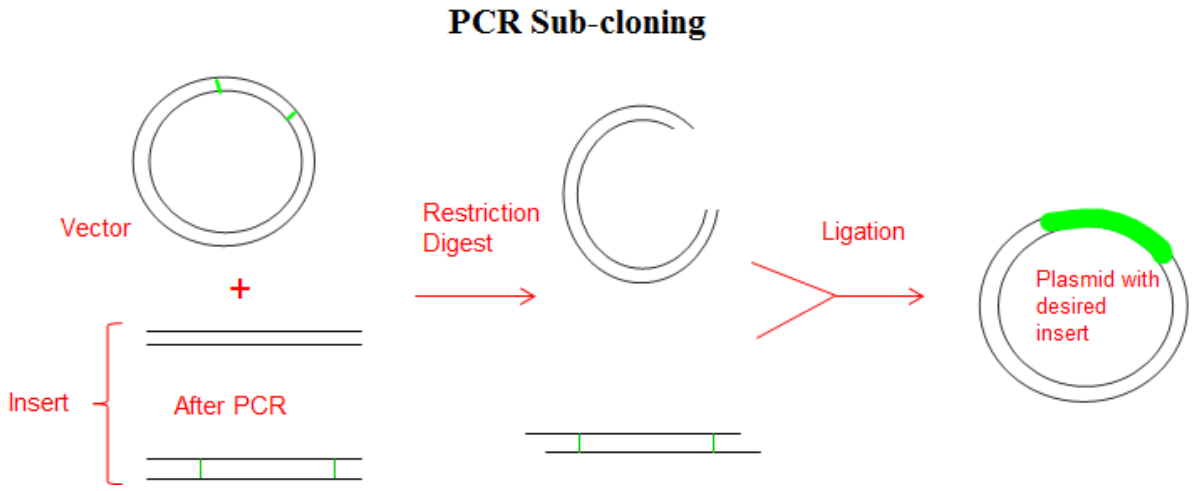

Figure 2.3: The sub-cloning of the human oxygenase domain for human iNOS. The insert was amplified using PCR, then both the vector and insert digested with the same restriction enzymes (HindIII and NdeI) and the insert ligated into the vector.

2.2.2 Digestion of Human iNOS to Obtain hiNOS$_{oxy}$

The human inducible nitric oxide synthase was digested with the HindIII restriction enzyme in order to separate the oxygenase domain in PcWori from the reductase domain. The mixture was placed in agarose gel 0.8 %, and the desired band cut and extracted from the gel using a gel extraction kit, "QIAGEN Gel Extraction Kit". The hiNOS$_{oxy}$ was self-circulated using the ligation kit (Ferments molecular biology tools). The 10x ligation buffer, 10 mM ATP, T4 DNA ligase, and MQH$_2$O were added to the hiNOS$_{oxy}$ and incubated overnight at room-temperature.

2.2.3 Digestion of Human iNOS to Insert into PET30a (+) Vector

The next step involved digesting both the insert hiNOS$_{oxy}$, to get rid of the reductase domain, and the PET-30a (+) vector, to open up the plasmid. The hiNOS$_{oxy}$ was digested with Nde I and Hind III. An agarose gel was run and the desired band was cut out from the gel and extracted using the

protocol given in the "QIAGEN Gel Extraction Kit". The hiNOS$_{oxy}$ (insertion) then inserted in a PET-30a (+) vector digested with the same restriction enzymes.

2.2.4 Electroporation

The ligation mixture was transferred by electroporation and expressed into *E. coli* XL 1 Blue competent cells. The mixture was placed into a water bath shaker for one hour to recover the cells and to allow expression of the resistance marker. The cell cultures were then plated on Lysogeny broth (LB) plates containing the proper selective marker gene, antibiotic resistance gene, for hiNOS$_{oxy}$, ampicillin. The plates were incubated for 16 hours at 37 ºC.

2.2.5 Cell Culture and Plasmid DNA Isolation

The plates that incubated for 16 hours contained colonies. A select number of isolated colonies were taken from the plate using a toothpick and transferred into a test tube of LB media supplemented with ampicillin. All equipment was sterilized, using an autoclave, and the work was done aseptically. Then, the test tube was incubated and shaken at 37 ºC overnight in a water bath. The last step was to purify plasmid DNA from the overnight culture using a mini-prep Kit (Ferments molecular biology tools). The DNA obtained was then sent for DNA sequencing to The Centre for Applied Genomics (TCAG), Toronto.

2.2.6 Ligation Experiment

A ligation experiment was proposed to ligate hiNOS$_{oxy}$ DNA inserted into the PET-30a (+) vector. Successful ligation should involve a 10x ligation buffer, 10 mM ATP, T4 DNA ligase, MQ H_2O, the insert, and the vector. The total volume of the ligation mixture was 20 µL; the mixture was incubated at 16 ºC overnight and then it was inactivated by heat at 75 ºC for 15

minutes. After that, the whole mixture was run on agarose gel 0.8% and gel extracted using a gel extraction kit "QIAGEN Gel Extraction Kit". The digestions were done for hiNOS to check the quality of our templates. The ligation mixture was subsequently transferred by electroporation into competent *E. coli* cells, plated and purified using the mini-prep kit, Ferments molecular biology tools.

2.2.7 The Sub-cloning Strategy of Human eNOS and nNOS Isoforms

The human eNOS-pBluescript (6577bp) and human nNOS-Bluescript (7290bp) were used as template to insert into PET-30a (+) vector and PET-28a (+) vector. The heNOS and hnNOS in pBluescript I and II SK (-) were obtained from the laboratory of Dr. Philip Marsden at the University of Toronto. The genes of interest, heNOS and hnNOS, were amplified in a regular PCR, using Pyrococcus woesei (PWO) polymerase kit (Roche), a 10x PWO buffer with $MgSO_4$, a human DNA template, MQH_2O, dNTP, and a forward and a reverse primers (Figure 2.2). The RF primers were designed specifically for this experiment, so in the end, no ligation step was needed. The reverse and forward primers of heNOS were used to amplify the coding region from methionine (Met) 1- isoleucine (Ile) 490. While the primers for hnNOS were used to amplify the coding region from methionine (Met) 1- threonine (Thr) 724. The PCR fragment obtained from the first PCR, PCR product, was considered to be a pair of primers. After amplification, PCR was applied again using the fragment obtained from the PCR. The PCR product was used as a primer in a linear amplification around circular plasmid PET-30a (+), dNTP, expand high fidelity buffer with Mg^{+2} (10X), water, and expand high fidelity polymerase (Roche). Once the primer annealed to the vector of interest, it extended in a linear amplification reaction around the circular vector. The PCR cycle was repeated 35 times. Time was considered in the third step

(elongation) in which PCR was extended to 2 minutes/kb. The PCR product was then run in 1% agarose gel. The last step was to digest by DpnI to cleave methylated parental DNA (Figure 2.4). The reaction mixture was then transferred into electro-competent cells (XL 1 Blue) and spread on LB plates containing the antibiotic kanamycin for heNOS. Results were checked with some restriction enzymes (*SmaI, EcoRI, NdeI,* and *NdeI+EcoRI*). The same protocol was followed with hnNOS, except slightly differently, as the vector was (PET-28a (+)) and the primers.

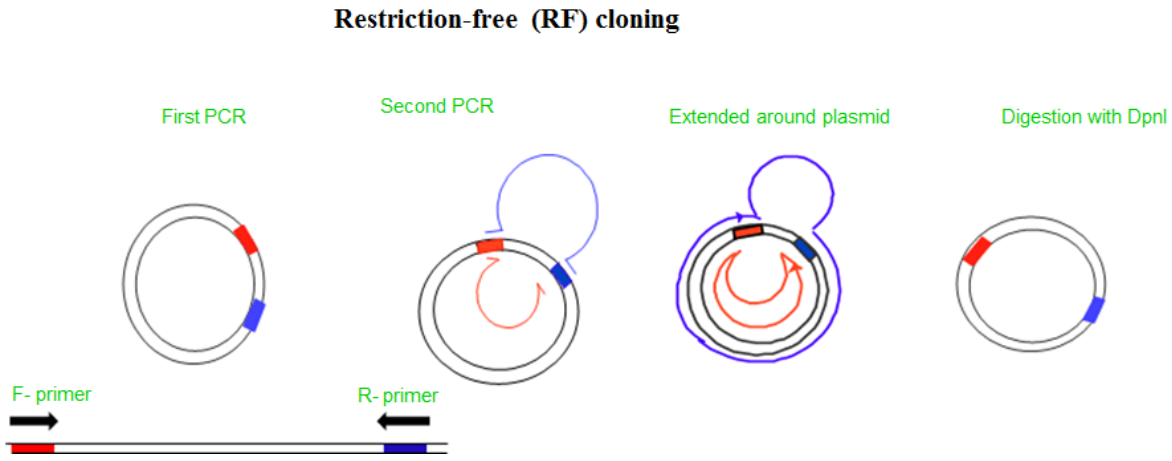

Figure 2.4: The RF cloning for human eNOS and human nNOS. Amplified the insert with specific primers by PCR, and then used the PCR product as primers to extend around the plasmid. The parental fragment was cut out using DpnI restriction enzyme. Figure 2.4 is derived from (Van den Ent and Lowe, 2006).

2.3 Results

2.3.1 PCR Mutagenesis of Human iNOS Oxygenase Domain

PCR mutagenesis was performed by two stop primers at the carboxyl end of the human iNOS oxygenase domain (Figure 2.5). The PCR experiment produced also an amplified oxygenase domain of hiNOS using PFU polymerase. In agarose gel, hiNOS isoform band was visualized

under ultraviolet (UV) light. The agarose gel shows that the reaction was successful in producing an amount of hiNOS$_{oxy}$ with the expected length of 1340 base pair (bp), data not shown.

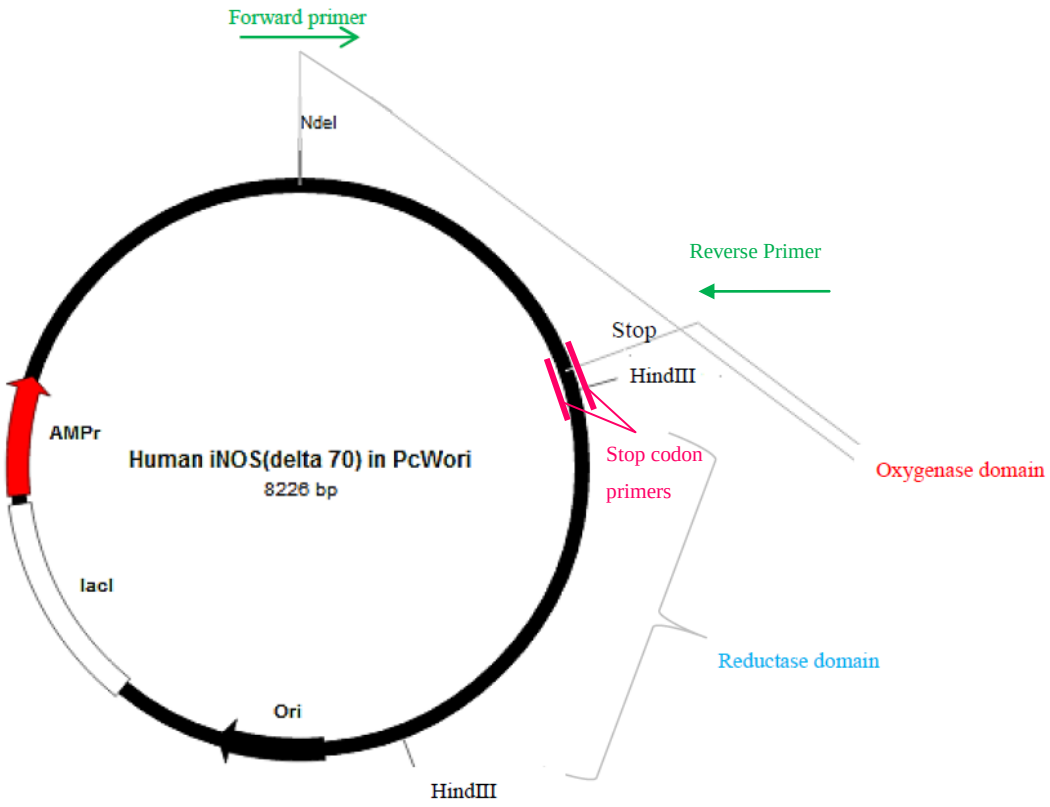

Stop codon forward primer hiNOS

5' CGAGAAGCGGAGAGACCCTGATAAGCTTCCATTGAAAGTCTTG 3'

Stop codon reverse primer hiNOS

5' GCTTTGACCAAGATTTCAATGGAAGCTTATCAGGGTCTCCGCTT 3'

Figure 2.5: Plasmid map of human iNOS (delta 70) in PcWori. A stop codon and a second HindIII site was introduced by the stop codon forward and reverse primers at the carboxyl end of the oxygenase domain. This figure also shows the forward and reverse primers used for sub-cloning the oxygenase domain.

Human iNOS (delta 70) in PcWori was digested after mutagenesis with Hind III. Figure 2.6 shows two bands which present both domains, the oxygenase domain and reductase domain. The target band, the oxygenase domain ($hiNOS_{oxy}$), is the larger band on the gel. The oxygenase band was cut out from the gel, extracted and ligated. Figure 2.7 shows the ligation product at the expected size and without reductase domain 6300 bp.

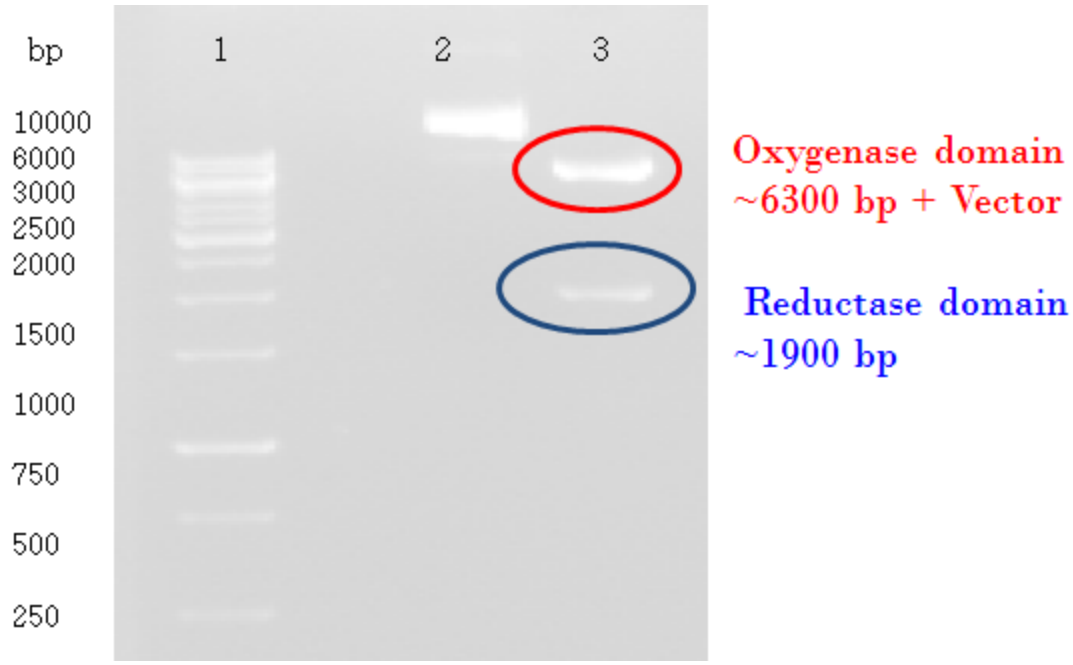

Figure 2.6: Mutated human iNOS plasmid digested by HindIII to obtain the $hiNOS_{oxy}$ and separated on 0.8% agarose gel. Lane 1: 1Kilobase DNA ladder, Lane 2: hiNOS (control/ undigested), Lane 3: hiNOS digest with HindIII**.**

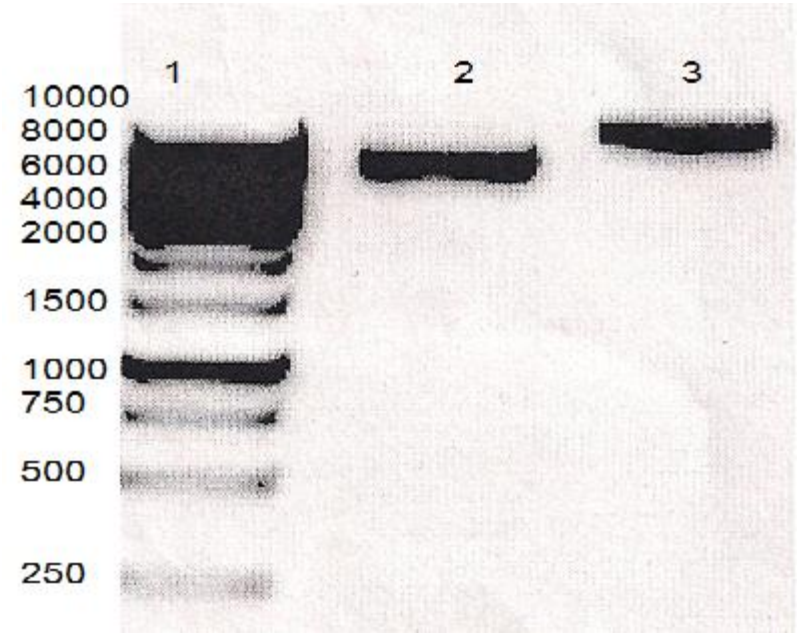

Figure 2.7: Self-circulated of Human $iNOS_{oxy}$. Lane1: 1Kilobase DNA ladder, Lane2: hiNOSoxy, without reductase domain, of length 6300 bp, Lane 3: the original hiNOS with both domains, control, of length 8226bp.

2.3.2 Sub-cloning of Human iNOS Oxygenase Domain

Two steps were performed to transfer the $hiNOS_{oxy}$ to the PET-30a (+) vector. First, the PCR amplified DNA was digested with two restriction enzymes, HindIII and NdeI, and used for ligation into PET-30a (+) vector (Figure 2.8). Second, the big fragment of PET-30a (+) (~ 5149bp) and the small fragment of hiNOS (~ 1340bp) were cut out from the gel and extracted by using the "QIAGEN Gel Extraction Kit". The products were confirmed by certain restriction enzymes as used to analyse purified plasmid. These enzymes specifically digest the DNA at certain short sequences.

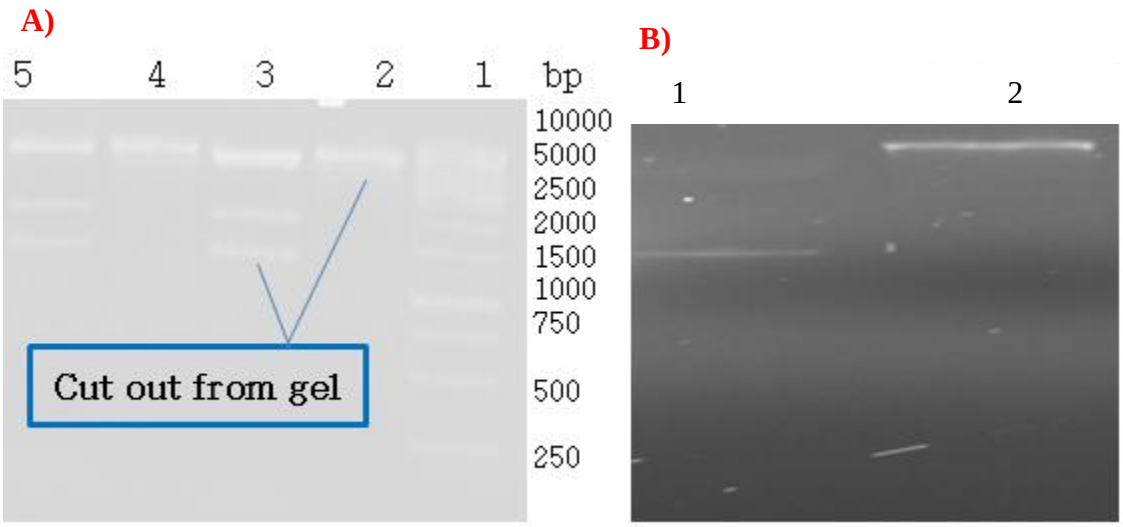

Figure 2.8: Digestion of HiNOS$_{oxy}$ by both HindIII and Nde I. A) Lane 1: 1Kilobase DNA ladder, Lane 2 and 4: the PET-30a (+) vector was digested by the restriction enzymes HindIII and NdeI and ended up as the expected size (~ 5149bp), Lane 3 and 5: hiNOS$_{oxy}$ was digested by the same restriction enzymes, resulting in the expected sizes (~ 5000- 1900-1340bp). **B)** Lane 1: hiNOS$_{oxy}$ fragment after been cut out from gel and extracted, Lane 2: PET30a (+) fragment after been cut out from gel and extracted.

2.3.3 Ligation of the Fragment of Human iNOS oxygenase domain into PET Vector

Both the hiNOS$_{oxy}$ and PET30a (+) were digested by HindIII and NdeI, the desired fragments were cut out from the gel and extracted using the "QIAGEN Gel Extraction Kit". The fragments were then run on agarose gel again to check that concentration levels remained suitable (Figure 2.8, B). The ligation step was not easy to achieve as many attempts were made to insert the digested fragment into PET-30a (+) vector. A variety of conditions were attempted including different ratios- (insert:vector) (1:1, 3:1 and 5:1), different temperatures (22 ºC, 16 ºC, and 4 ºC) , and different times (overnight, 2 hours, and 5 hours) before finding that 5:1 and 16 ºC overnight worked best (Table 2.1), data not shown. Target genes were cloned in PET plasmids under the control of bacteriophage T7 transcription, so that high yields of the desired product could be obtained.

Table 2.1: Different ratios used in the attempted ligation of the PCR fragment of hnNOS into the vector

Content	Quantity			
$hiNOS_{oxy}$ (PCR product)	0 µL	10 µL	9 µL	15 µL
Vector PET30a (+)	5 µL	10 µL	3 µL	3 µL
T4 DNA ligase buffer, 10x conc	1 µL	1 µL	1 µL	1 µL
ATP (10mM)	1 µL	1 µL	1 µL	1 µL
MQH_2O	12.5 µL	0 µL	5.5 µL	0 µL
T4 DNA ligase	0.5 µL	0.5 µL	0.5 µL	2.5 µL

2.3.4 Cell Culture and Plasmid DNA Isolation

After mini-prep, which was used to isolate and purify our DNA from an overnight-transformed *E. coli* culture, the product was analyzed by gel electrophoresis. The target DNA was sequenced to verify that there were no spontaneous mutations. The desired plasmid was then ready to use in the protein expression process.

2.3.5 The Sub-cloning of Human eNOS and Human nNOS

Initially, the same protocols used for hiNOS (PCR, digestion, extraction, and ligation) were applied for heNOS and hnNOS, but unfortunately they did not work. That led us to use of the PCR technique with RF cloning (Figure 2.4) which is a simple method to insert a DNA fragment into any vector without the need for restriction sites and ligation. This experiment was

successful, showing in the gel expected amplified fragments at expected size or length without any apparent non-specifically amplified DNA (Figure 2.9). Human eNOS was fully verified by sequencing, which is usually done on DNA samples before proceeding to further steps. For human nNOS, sub-cloning using the primers was successful, as shown by gel electrophoresis (Figure 2.9). Unfortunately, several attempts were made to extend the liner amplification of hnNOS (the PCR product) around the PET28a (+), but they did not work.

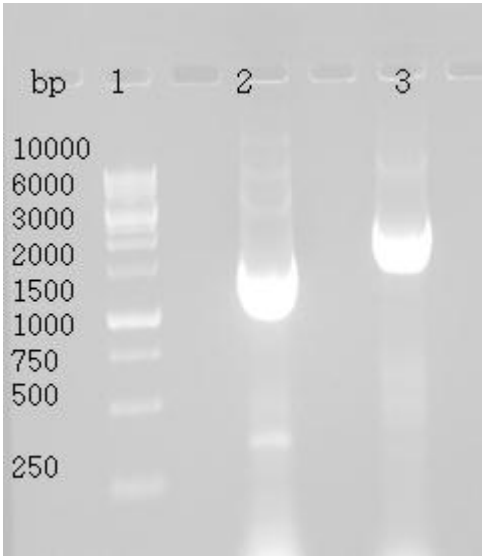

Figure 2.9: Agarose gel electrophoresis (1.0%) of the PCR amplified linear fragments for heNOS and hnNOS using high fidelity polymerase. Lane 1: 1Kilobase DNA ladder, Lane 2: heNOS ~ 1500bp, Lane 3: hnNOS ~ 2000 bp.

2.4 Discussion and Summary

In summary, having a vector that contains only the oxygenase domain is preferential for use as an over expression vector. A series of procedures were modified and were used in our attempts to insert desired gene products into suitable vectors for *E. coli* expression: PCR, restriction enzyme digestion, ligation, agarose gel electrophoresis, gel extraction, and transformation into *E.*

coli. DNA sequencing techniques can characterize DNA thoroughly; however, restriction enzyme analysis is a basic molecular technique as it is ideal for initial and fast sequence screening (Tiong *et al*., 2010). The restriction enzymes were used in this project to confirm the obtained PCR products. The primers used in the PCR were designed (1) to amplify the desired region of the gene, and (2) to provide restriction endonuclease recognition sites to help in the sub-cloning of the amplified fragments. Achieving our results was not an easy task. Amplifying the desired region of human NOS was challenging as we had to design several primers and to change the PCR conditions, for example, the annealing times or even the extension times. The ligation of the PCR product to the vector was also difficult as enormous effort was made to find a suitable temperature, time, and optimal ratio (see Table 2.1). We tried also to desalt the samples, PCR products, using a nitrocellulose filter prior to the electroporation to increase the ligation success rate, but these attempts were unsuccessful. The ligation of hiNOS_{oxy} into the PET vector did not work because the restriction enzyme NdeI may have difficulty cutting near the end of a linear fragment. In order to avoid using ligation, RF cloning was chosen for heNOS and hnNOS as it requires no ligation step. This technique worked for heNOS but not for hnNOS. The forward and reverse primers for human nNOS were designed with an NdeI site at the 3' end, a site that included the start TATG and the reverse primer encoded an EcoRI recognition site GAATTC (Figure 2.2). These primers were specifically designed to insert the hnNOS into the PET28a (+) plasmid; however, our attempts to clone hnNOS did not succeed. Human nNOS or the plasmid itself may not be clean enough or is contaminated and need of further purification. It was therefore decided to stop dealing with hnNOS and move on to the next part of the project, protein expression, working only with human iNOS and human eNOS.

Chapter 3

Purification and Characterization of the Human NOS Recombinant Oxygenase Domain Proteins

3.1 Introduction

This chapter explains the techniques for development of an expression system for the human NOS proteins in PcWori vector and PET vector, starting with the DNA obtained and finishing with the purified protein products. All proteins were expressed and purified in the dimers form as all isoforms are active only in the dimeric state.

The yield of protein is proportional to *E. coli* cell quantity. Therefore, the growth media is an important component of the expression systems. Examining the bacterial culture is also useful in optimizing the production of our recombinant protein. Optical density (OD_{600}) of 600 nm wavelength light is the most common way to estimate *E. coli* cell density. An OD_{600} = 0.8 to 1.0 usually means that the cells have reached the exponential growth phase. At this point, the vast majority of *E. coli* cells are alive and healthy and are in an ideal state to produce or express protein. An OD_{600} higher than 1.0 means the *E. coli* cells are entering the death phase and the culture consists of dead cells resulting in higher protein degradation. Generally, the OD_{600} value is an important indicator of the proper time to induce protein expression in *E. coli*.

A variety of chromatographic methods were commonly used to try and purify the recombinant proteins. The protein was then analyzed by using absorbance spectroscopy. These approaches were all used in the purification and characterization of our recombinant proteins.

3.2 Experimental Techniques

3.2.1 Electroporation

The $hiNOS_{oxy}$ was cloned into the ampicillin resistance gene (Amp^r) to produce $hiNOS_{oxy}$ in PCWori. The $hiNOS_{oxy}$ was transferred by electroporation into *E. coli* BL21 (DE3) cells, using the same protocol that was described previously. Culturing the cells was the next step and, once again, using the same protocol mentioned above but with slight variations, in that a well-isolated colony was added to 50 mL LB media supplemented with 50 µL ampicillin antibiotic and placed in a sterile 250 mL Erlenmeyer flask instead of a test tube. The mixture was placed into a water bath shaker overnight to recover the cells and allow expression of the resistance marker. For human $eNOS_{oxy,}$ the same protocol used with $hiNOS_{oxy}$ was employed, except that the kanamycin resistance gene (Kan^r) was used instead of Amp^r because the $heNOS_{oxy}$ gene is in the PET30a (+) vector.

3.2.2 Protein Expression

For $hiNOS_{oxy}$, two sterile Erlenmeyer flasks, each one containing 1 L of terrific broth (TB) media supplemented with 100 µg/mL of ampicillin antibiotic were prepared. Then 10 mL of overnight culture were added to each of the Erlenmeyer flasks. The flasks were placed in a shaking incubator at 200 rpm at 37 ºC for about 3 hours until optical density ($O.D_{600}$) of 0.8-1.0 was reached. Protein expression was induced by adding 500 µM of isopropyl β-D-1-thiogalactopyranoside (IPTG), 400 µM of δ-aminolevulinic acid (δ-ALA), 100 mg of riboflavin, and 250 µL of trace metals (Spratt, 2008). After this step, the temperature was lowered to 25 ºC, and the flasks were placed in the shaker for another 40 hours, as the *E. coli* cells grew more

slowly after protein induction. Samples were taken every four hours during the 40 hour-expression to check the highest level of expression time by SDS-PAGE gel. The final step in this process is harvesting the cells, using a centrifuge (in a SLA-3000 rotor) at 10 000 rpm, 4 Cº for 8 minutes. The cells then were ready to flash freeze on dry ice and store at –80 ºC in a falcon tube.

For human $eNOS_{oxy}$, the same method but with several modifications was used for expressing $heNOS_{oxy}$. LB media was used instead of TB media in two sterile Erlenmeyer flasks, each one containing 1 L of the media supplemented with 30 µg/mL of kanamycin antibiotic. These 1L cultures were grown at 37 ºC, 200 rpm until an O.D. at 600 nm reached 1. Expression of the protein was induced by adding 500 µM IPTG and harvested after 4 hours by centrifugation using the same conditions described previously (Rafferty *el al*., 1999). Samples were taken each hour during the expression period.

3.2.3 Cells Lysing by Homogenizer

An Avestin EmulsiFlex-C5 homogenizer (Ottawa, ON) machine was used to break/open the cells and isolate the plasmid. The first step involved thawing the cells on ice and resuspending them in 200 mL of lysis buffer. The lysis buffer consisted of 40 mM Tris-HCl, pH 7.5, 10 % glycerol, 150 mM NaCl, 1 mM L-arginine (to stabilize the protein), 3 mM ascorbic acid, 10 µM H_4B (to stabilize the dimer), 1 mM PMSF (to avoid degradation the protein), and one pill of protease inhibitor cocktail tablets containing leupeptin, aprotinin, and peptstatin (protected from the presence of proteases during the purification). In the second step, the cells were lysed by the homogenizer. The lysed cells were centrifuged in a SS-34 rotor at 20 000 rpm for 30 minutes at 4 ºC. The pellet was discarded, while the supernatant was used for the following protocol.

3.2.4 Protein Purification and Metal Chelation Chromatography

Many proteins have the ability to bind to specific molecules tightly, and since our protein contain a poly-histidine tag, the protein were purified using ammonium sulphate precipitation, followed by metal chelation (Ni^{+2}) chromatography. The desired protein was bound to the resin, whereas other substances were washed through the column. The protein could then be eluted by washing the column with a solution containing a high concentration of a free ligand (imidazole). This experiment must be carried out at 4 ºC.

The protocol for purifying hiNOS_{oxy} in PcWori followed that previously published by (Ghosh *et al*., 1997), with a few modifications. Ammonium sulphate was added to 35 % to clarified the supernatant, stirred for 45 minutes, and then centrifuged (in a SS-34 rotor) at 20 000 rpm for 30 minutes at 4 ºC. After that, the pellet was discarded, while 55 % of the ammonium sulphate was added to the supernatant, once again stirred for 45 minutes and centrifuged. The ammonium sulphate pellets were then resuspended in 100 mL of pellet buffer consisting of 40 mM Tris-HCl, pH 7.5, 10 % glycerol, 1 mM L-arginine, 250 mM NaCl, and 1 mM PMSF. Before the protein was added to the Ni^{2+}- immobilized metal ion affinity chromatography (IMAC) resin, the resin was charged with metal ions. The column was washed with 3 column volumes of 0.1 M $NiSO_4$ followed with 5 column volumes of distilled water to remove excess metal ions. The column was washed with another 5 column volumes of pellet buffer, then the resuspended ammonium sulphate pellets were mixed with the charged Ni^{2+} resin slowly for one hour. The mixture was then poured back into the column and allowed to rest for 30 minutes. The column was washed with 5 column volumes of pellet buffer followed by 5 column volumes of 20 mM imidazole dissolved in 100 mL of pellet buffer. The Human iNOS_{oxy} protein was then eluted by 50 mM

imidazole dissolved in 100 mL of pellet buffer and collected in 5-6 mL fractions. The eluted fractions were poured into dialysis tubing and dialyzed against one L of Dialysis Buffer #1 (50 mM Tris-HCl, pH 7.5, 10 % glycerol, 5 µM L-arginine, 250 mM NaCl, 1 mM DTT, 4 µM H_4B, 3 mM ascorbic acid, and 0.1 mM PMSF). After 3 hours at 4 ºC, the protein was transferred into one L of Dialysis Buffer #2 (50 mM Tris-HCl, pH 7.5, 10 % glycerol, 5µM L-arginine, 100 mM NaCl, 1 mM DTT, 4 µM H_4B, 3 mM ascorbic acid, and 0.1 Mm PMSF) and left to dialyze overnight at 4 ºC (Spratt, 2008). The human $iNOS_{oxy}$ protein was concentrated using a Vivaspin 15-maximum spin speed and centrifuged (in a SS-34 rotor) at 10 000 rpm for 1 hour and 20 minutes at 4 ºC. After the desired concentration was reached, the purified human $iNOS_{oxy}$ protein was aliquoted, flash frozen on dry ice, and stored at -80 ºC for further purification.

3.2.5 SDS-PAGE and Spectroscopic Analysis

Sodium dodecyl sulfate polyacrylamide gel electrophoresis is a technique widely used to check protein purity and size. Therefore, the collected fractions from the Ni^{2+}-column were verified using a 10 % SDS-PAGE. First, the gels were prepared with 5 mL of 30 % acrylamide, 7.5 mL of separating gel, and 2.5 mL of distilled water. The mixture was degassed for 5 minutes. After degassing, 10 % of ammonium presulfate (APS) (100 mg/mL) and 10 µL of tetramethylethylenediamine (TEMED) were added to increase polymerization efficiency were poured between two glass plates. The stacking gel was prepared with 0.65 mL of 30 % acrylamide, 2.5 mL of separating gel, and 1.85 mL of distilled water. The mixture was also degassed, and 10% of APS (100 mg/mL) and 10 µL of TEMED were added to it. Then the mixture was poured on the top of the separating gel using a comb in order to prepare the loading wells. Our samples were prepared, and 10 µL of each sample were mixed with a 4x loading dye

and heated in a water bath at 80 ºC for 15 minutes. The samples were loaded onto the gel. The gel was stained with Coomassie blue dye. The purified protein was also scanned on a Varian Cary (Varian, Mississauga, ON) at wavelengths between 300 -700 nm, to monitor the soret absorbance peak that occurs at around 400 nm. The concentration of the human iNOS was determined using the ε_{397} of 72 mM^{-1} cm^{-1} (Spratt, 2008).

3.2.6 Gel Filtration Chromatography

Gel filtration chromatography was used for further purification after the protein was obtained from the metal chelation column. Gel filtration (Superdex 200 10/300 GE column) was suitable for the separation of monomers from dimers and from contaminants of lower molecular weight. The AKTApurifier (GE) chromatography system was run at a flow rate of 1 mL/min, to insure that the pressure did not go too high with the increase in flow rate, and the wavelength was set at 405 nm to detect the heme; 215 nm to detect peptides, and 280 nm to detect both tyrosine and tryptophan residues. All the buffers in this experiment had to be filtered and degassed prior to use to prevent air bubbles into the resin. The column was first washed with degassed distilled water, followed with 200 mL of 0.5 M sodium hydroxide, 200 mL of 0.5M acetic acid, and then 25 mL distilled water, again followed by 50 mL 0.075 M of sodium phosphate. Second, the column was calibrated by using a protein molecular mass kit containing blue dextran, beta-amylase, alcohol dehydrogenase, and bovine serum albumin. Third, the buffer contained 0.02 M of sodium phosphate buffer, pH 7.5 and 0.15 M of sodium chloride was applied to the column. Finally, the sample, $hiNOS_{oxy}$, was applied using a 0.3 mL syringe. We tried the gel filtration with decrease the flow rate to 0.5 ml/min to improve the purity of protein. This experiment must

be carried out at 4 ºC. Once again, the 10 % SDS-PAGE was used to monitor the eluted fractions.

3.3 Results

3.3.1 Protein Expression

The plasmid was tested for the production of hiNOS$_{oxy}$ protein expression under many different conditions, such as the period of incubation, temperature, speed of the shaker, and the concentration of IPTG used for induction. A successful expression of hiNOS$_{oxy}$ (Figure 3.1) was achieved after 40 hours of incubation, at 25 ºC and 200 rpm. The expression was attained also by using TB medium, because it is rich of nutrient medium which supports *E. coli* growth to the desired OD$_{600}$. For human eNOS$_{oxy}$, it was evident that the production of protein was extremely low when tested using SDS-PAGE (data not shown).

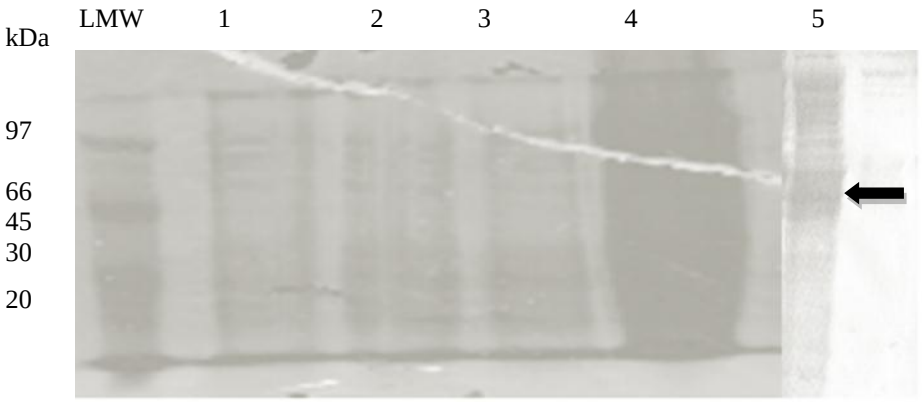

Figure 3.1: SDS-PAGE analysis of the human iNOS oxygenase domain. Expression and purification of target proteins from culture induced by 500 mM IPTG with 40 hours expression. Lane 1: protein expressed after 10 hours, Lane 2: after 12 hours, Lane 3: after 24 hours, Lane 4: after 40 hours, Lane 5: lysis the cells after 40 hours. The arrow indicates the hiNOS$_{oxy}$ at expected size, ~ 48 kDa.

3.3.2 Protein Purification and Metal Chelation Chromatography

The purification by metal (nickel) chelation chromatography column is a suitable method for a first step to gain a pure protein. The proteins bind to the resin, and then eluted from the column by washing with a buffer containing a high concentration of imidazole. Figure 3.2, SDS-PAGE 10 % shows proteins isolated from each step of the purification procedures. Lane 12 shows that only one band at expected size ~ 48 kDa is formed in the final elution step from the metal chelation chromatography column. Moreover, the protein was characterized by absorbance spectroscopy, UV-visible spectrum, which was used to determine protein concentration, Table 3.1.

Table 3.1: The yield of protein ($HiNOS_{oxy}$) per liter after purificatin by nickel chelation chromatography.

Protein $HiNOS_{oxy}$	Concentration	Protein Yield (mg/2 L media)
Trial #1 obtained (1.5 mL)	3.6	0.27
Trial #2 obtained (14 mL)	3.20	2.2
Trial #3 obtained (1.5 mL)	4.4	0.30
Trial #4 obtained (7 mL)	2.70	0.94

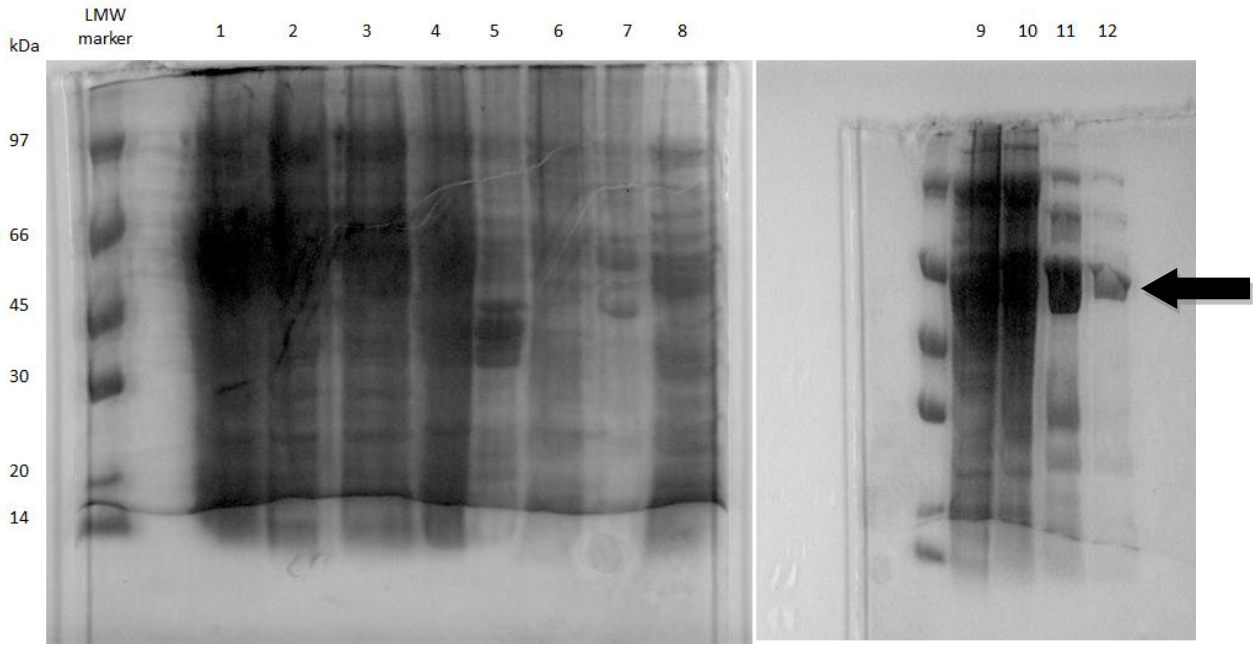

Figure 3.2: SDS-PAGE of hiNOS$_{oxy}$ purification and the fractions containing hiNOSoxy that were eluted off the Ni2+ column: Lane 1: pellet after lysis, Lane 2: supernatant after lysis, Lane 3: pellet 35% $(NH_4)_2SO_4$, Lane 5 and 4: supernatant of 35% $(NH_4)_2SO_4$, Lane 6: pellet 55% $(NH_4)_2SO_4$, Lane 7: supernatant after 55% of $(NH_4)_2SO_4$, Lane 8: flow through, Lane 9 and 10: pellet buffer wash, Lane 11: 20 mM of imidazole, Lane 12: 50 mM of imidazole. The arrow indicates the desired protein.

3.3.3 Gel Filtration Chromatography

Gel filtration chromatography is a unique method among other chromatographic methods. It does not damage proteins when they pass through the column because they do not bind to the resin. This method is useful for determining the presence of the dimer form under non-denaturing conditions, in contrast to the denatured and conditions that arises with SDS-PAGE. Human iNOS$_{oxy}$ was purified and analyzed using gel filtration. This experiment is extremely important as ITC will be the next experiment and requires a pure and dimeric protein. Gel filtration separates the protein based on size so that the heme containing hiNOS$_{oxy}$ (a dimer) is eluted earlier than the

non-heme (a monomer) protein. SDS-PAGE was used to check the protein's purity as shown in Figure 3.3. The fractions containing hiNOS$_{oxy}$ eluted off the column at a flow rate of 1 ml/min, as shown in Figure 3.4. The decreased of the flow rate to 0.5 ml/min improved the purity of hiNOS$_{oxy}$, as shown on Figure 3.5, which makes it clear that the protein is pure as there are no contaminating proteins visible.

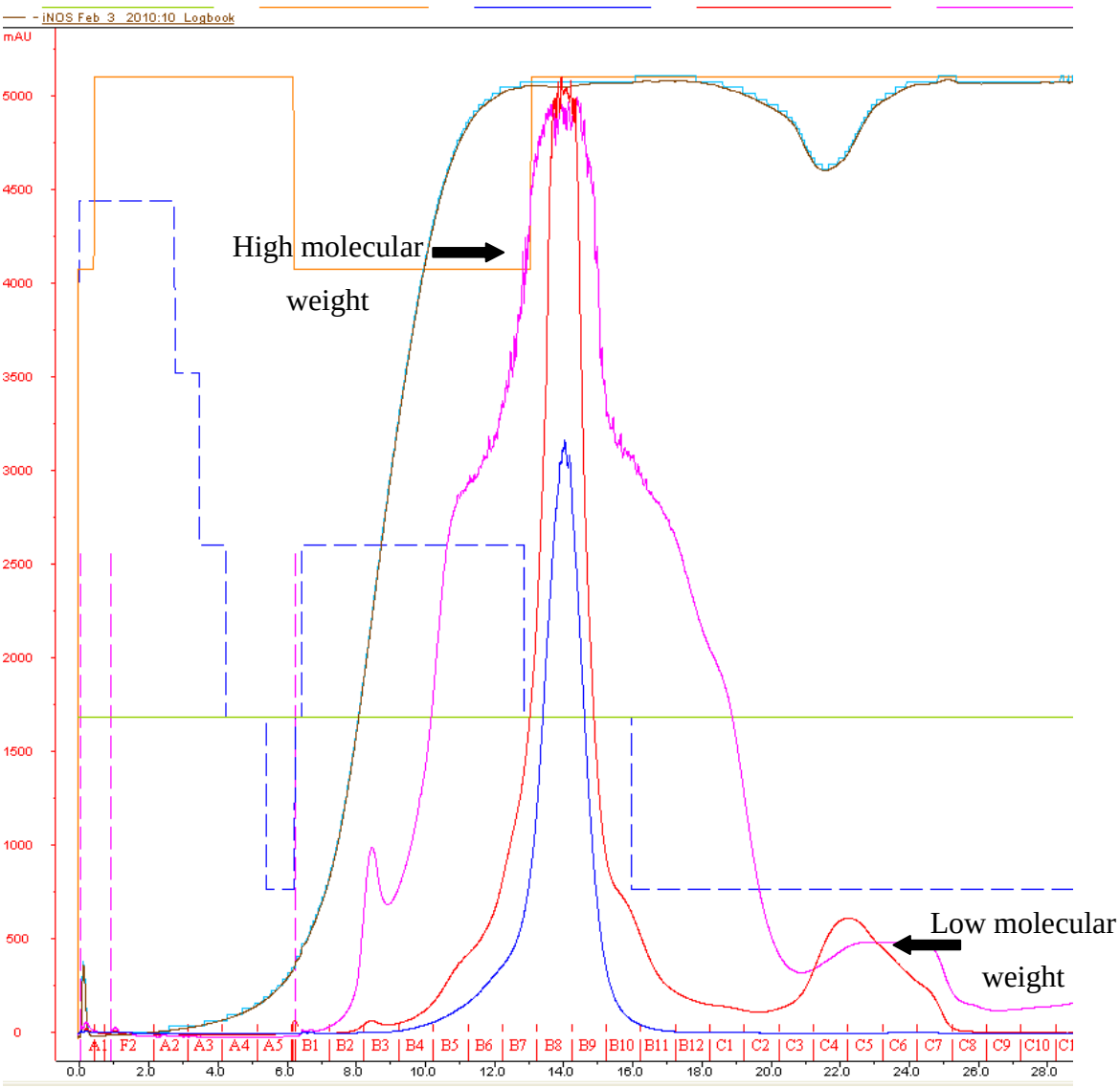

Figure 3.3: Gel filtration chromatography of hiNOS$_{oxy}$. The pink line indicates the absorbance at 215 nm (peptide bond). The blue line indicates the absorbance at 280 nm (mainly tyrosine and tryptophan absorbance), and the red line indicates the absorbance at 405 nm (heme- signifying hiNOS$_{oxy}$ domain). This figure makes clear the high molecular weight protein eluted first from the column, while the low molecular weight protein eluted last, as the two arrows indicate.

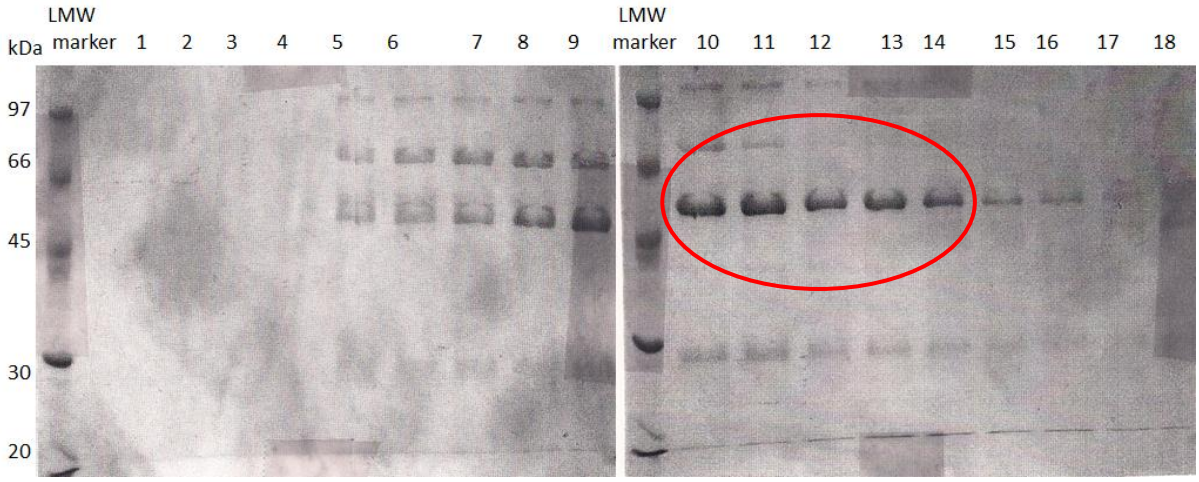

Figure 3.4: SDS-PAGE of hiNOS$_{oxy}$ purified by gel filtration. This gel shows the collected fractions during elution from (Superdex 200 10/300 GE) column. Lanes 1-4: resin wash; Lanes 5-9: the beginning of the protein elution, but contains high molecular weight contaminants, Lanes 10-14: fractions containing dimer hiNOS$_{oxy}$ that were eluted off the column at the correct size, as indicated by the circle; Lanes 15-18: resin wash.

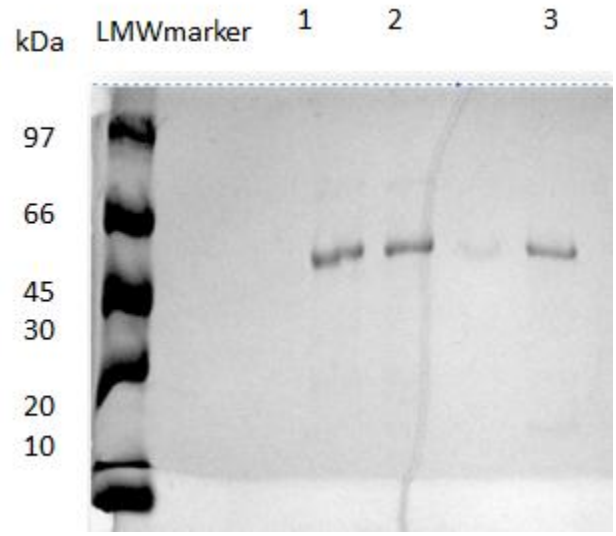

Figure 3.5: SDS-PAGE analysis of hiNOS$_{oxy}$ protein fractions isolated by gel filtration. This gel shows the increase of the protein purity when slowing the flow rate to 0.5 ml/min. Lane 1 to 3 are fractions containing hiNOSoxy dimer that were eluted off the column.

3.4 Discussion and Summary

The human $iNOS_{oxy}$ (delta70) vector carries a deletion of the first 70 amino acids and the N-terminal poly-histidine in the PcWori vector. This vector was expressed into *E. coli* BL21 (DE3) cells to minimize the proteolysis of $hiNOS_{oxy}$ during the expression process. Protein denaturing due to proteolysis can be a problem during the purification of the protein; however, it is most likely to occur after cell lysis, which disrupts the cellular organization and releases proteases. To limit the denaturing of our protein, a mixture of inhibitors such as leupeptin and pepstain were used in order to insure that all types of proteases were inhibited. Carrying out the purification experiments at 4 ºC has advantages in that it helps to reduce the activity of proteases. Pure recombinant histidine-tagged protein was obtained using metal (Ni^{2+}) chelation chromatography and the protein was eluted using an imidazole gradient. Imidazole is suitable when the expressed protein is unstable or denatured. Unlike metal chelation chromatography, gel filtration of proteins does not involve binding to the chromatography medium. It separates proteins according to differences in size as they pass through a resin. Samples with a very large molecule such as blue dextran go through the pores very quickly. Meanwhile, proteins with small molecules, such as bovine serum albumin, take more time to elute from the column. According to the concept of this technique, we observed that the dimer, a large protein, was eluted from the column first, while the non-dimer was eluted from the column second. The protein should be free of imidazole after gel filtration. The best results for high resolution fractionation from the gel filtration were achieved with samples that were partially purified by other types of chromatography, such as metal chelation chromatography (Montgomery, 2009). The dimer form of the protein was our goal because dimerization is essential for catalytic activity.

Chapter 4

Summary and Future Considerations

4.1 Summary

The polymerase chain reaction was used to amplify the coding region for the oxygenase domain of the human NOS enzymes. Attempts were made to insert the amplified fragments into the proper vector. The protocols used in this project (Figure 2.3 and 2.4) involve the sub-cloning of the oxygenase domain of the three human NOS isoforms. Successful sub-cloning and expression were difficult to achieve, as a series of *E. coli* expression plasmids for the oxygenase domain were used in the investigation. Human NOS was purified using metal chelation chromatography, as the NOS protein expressed includes a coding region for a poly-histidine tag. Gel filtration was also used in this project for further purification process. The identities of the pure proteins were confirmed by using SDS-PAGE gel electrophoresis and absorbance spectroscopy. To gain a high yield of protein, it was worthwhile to test the vector, insertion, and culture conditions to reach optimal results. The development of this expression system needed many modifications as these steps are highly sensitive and many options were available at each step, so any small change might affect the results or the overall yields. Investigation of inhibitors that bind tightly to the active site of the human NOS_{oxy} enzyme is the main object of the early-stage of drug discovery. Unfortunately, figuring out the right conditions to gain the target protein took a lot more time than expected. However, gaining a protein is a very valuable goal because, in the case of mammalian protein (e.g. NOS enzymes), the extraction from a native source is not usually feasible due to extremely high costs and low yields. Therefore, it was important to develop the *E. coli* expression system in order to produce adequate amounts of protein.

4.2 Future Considerations

I. Select an inhibitor for the first round of trials with known biophysical properties and binding constants (e.g. 1400W and L-NMMA);

II. Model the active site with target ligand (inhibitor) in the core. Based on the composition and differences in the shells that are far away from the core/ active site residues, modifications/substituents will be modeled into the ligand molecule. Modification (i.e. bulky residues) will be incorporated onto the target ligand to exploit minor differences in those residues that may ultimately result in ligands with increased isoform selectivity;

III. Generate the modified ligands and pursue biophysical characterization of the ligand binding to the different isoforms, and

IV. Any modified ligands that show differential or increased isoform-specific binding will be incorporated into activity assays using the NOS holo-enzymes.

***Appendix A*:** A schematic representation of the PCR amplified human NOS_{oxy} protein containing a his 6 tail

***Appendix B*:** The forward and reverse primers for human eNOS and human nNOS amplification.

Primer Name	Sequence (5')	Tm (C°)	Unique RE Sites
eNoxFor	GCGGAATTCATATGCACCACCACCACCACCACATGGGCAACTTGAAGAGCGTGGCC	63	EcoRI, NdeI
eNoxRev	CAGGAAGCTTATCAGATGCCGGTGCCCTTGGCGG	70	HindIII
nNoxFor	GGAATTCATATGGAGGATCACATGTTCGGTG	55	NdeI, EcoRI
nNoxRev	ATCGATAAGCTTATCAGGTGCCTTTCCAGACATGCGTGTTCC	63	HindIII

Appendix C: Map of the PET 30a (+) vector containing the human iNOS oxygenase domain. The cloning of the hiNOS$_{oxy}$ domain was performed by amplifying the coding region found in a human iNOS expression vector supplied by Dr. Dipak Ghosh of Duke University. Two primers were used to amplify insert a stop codon immediately after the coding region of human iNOS gene from residue Leu 71 to Pro508 and do not include the calmodulin binding domain. The amino terminus has an NdeI site followed by 6 His residues before Leu71.

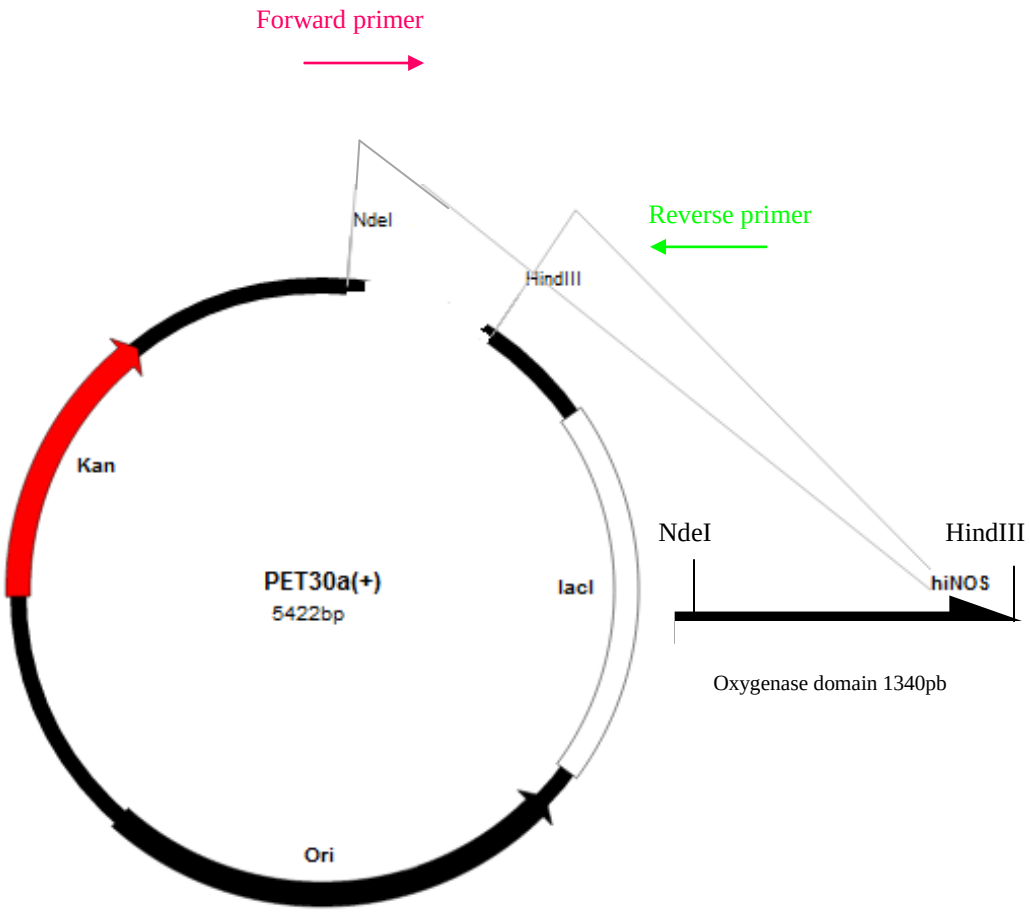

Vector **Insert**

Appendix D: Map of the PET 30a (+) vector containing the human eNOS oxygenase domain. The cloning of the $heNOS_{oxy}$ domain was performed by using human eNOS cDNA (PM831221) supplied by Dr. Philip Marsden of the University of Toronto. Two primers were used to amplify the coding region of human eNOS cDNA from residue Met1 to Ile490 and do not include the calmodulin binding domain.

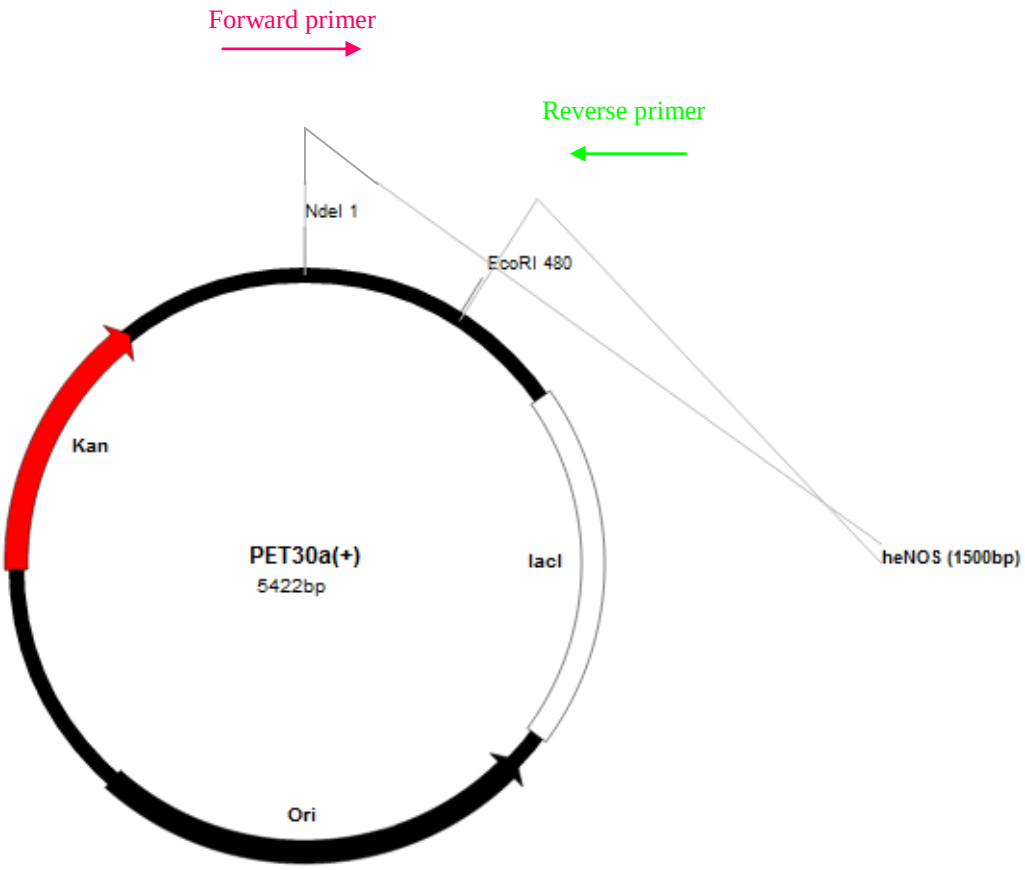

Appendix E : Map of the PET 28a (+) vector containing the human iNOS oxygenase domain. The cloning of the hnNOS$_{oxy}$ domain was performed by using human nNOS cDNA (MDN75-3'-5') supplied by Dr. Philip Marsden of the University of Toronto. Two primers were used to amplify the coding region of human nNOS cDNA from residue Met1 to Thr724 and do not include the calmodulin binding domain.

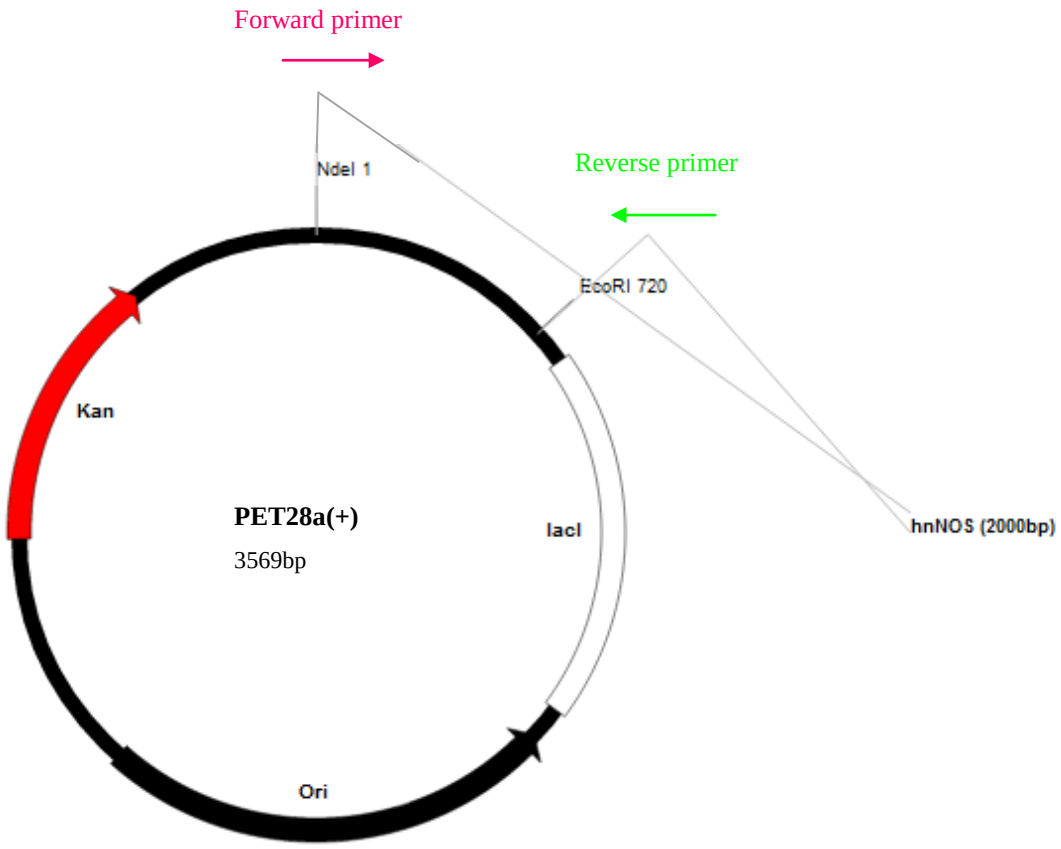

Bibliography

Adrian, R. M. (1999) Pulsed carbon dioxide and long pulse 10-ms erbium-YAG laser resurfacing: a comparative clinical and histologic study. *J Cutan Laser Ther* **1**, 197-202.

Alderton, W. K., Cooper, C. E. and Knwles, R. G. (2001) Nitric oxide synthases: structure, function and inhibition. *Biochem* **357**, 593-615.

Bauer, J. A., Booth, B.P., and Fung, H. (1995) Nitric oxide donors: Biochemical pharmacology and therapeutics. *Pharm* **34**, 361-381.

Boyhan, A., Smith, D., Charles, I. G., saqi, M. and Lowe, P. N. (1997) Delineation of the arginine- and tetrahydrobiopterin-binding sites of neuronal nitric oxide synthase. *Biochem* **323**, 131-139.

Crane, B. R., Arvai, A. S., Gachhui, R., Wu, C., Ghosh, D. K., Getzoff, E. D., Stuehr, D.,Tainer, J. A. (1997) The structure of nitric oxide synthase oxygenase domain and inhibitor complexes. *Science* **278**, 425-431.

Crane, B. R., Arvai, A. S., Ghosh, D. K., Wu, C., Getzoff, E. D., Stuehr, D. J., Tainer, J. (1998) Structure of nitric oxide synthase oxygenase dimer with pterin and substrate. *Science* **279**, 2121-2126.

Cooper, G. M. (2000) The cell: a molecular approach. Second Edition; Sinauer Associates: Sunderland, Chapter13.

Daff, S. (2010) NO synthase: structures and mechanisms. *Chem* **23**, 1-11.

De Azevedo WF Jr. and Dias., R. (2008) Experimental approaches to evaluate the thermodynamics of Protein-Drug interactions. *Curr Drug Targets* **9**, 1071-1076.

Di Giacomo, C., Sorrenti, V., Salerno, L., Cardil, V., Guerrere, F., Siracusa, M., Avitabile, M. and Vanella, A. (2003) Novel inhibitors of neuronal nitric oxide synthase. *Exp Biol Med* (*Maywood*) **228**, 486-490.

Fischman, T., Hruza, A., Niu, X., Fossetta, J., Lunn, C., Dolphin, E., Prongay, A., Reichert, P., Lundell, D., Narula, S. and Weber, P. (1999) Structural characterization of nitric oxide synthase isoforms reveals striking active-site conservation. *Nat Struct Biol* **6**, 233-242.

Fishlock, D., Guillemette, J. and Lajoie, G. (2002) Synthesis of syn and anti-isomers of trans-cyclopropyl arginine. *J Org Chem* **67**, 2352-1354.

Garcin, E. D., Arvai, A. S., Rosenfeld, R. J., Kroeger, M. D., Crane, B. R., Andersson, G., Andrews, G., Hamley, P. J., Mallinder, P. R., Nicholls, D. J., St-Gallay, S. A., Tinker, A. C., Gensmantel, N. P., Mete, A., Cheshire, D. R., Connolly, S., Stuehr, D. J., Aberg, A., Wallace, A. V., Tainer, J. A. (2008) Anchored plasticity opens doors for selective inhibitor design in nitric oxide synthase. *Nat Chem Biol* **4**, 700-707.

Garvey, E. P., Oplinger, J. A., Tanoury, G. J., Sherman, P.A., Fowler, M., Marshall, S., Hermon, M.F., Paith, J.E. and Furfine, E. S. (1994) Potent and selective inhibition of human nitric oxide synthases. Inhibition by non-amino acid isothioureas. *J Bio Chem* **269**, 26669-26679.

Geber, N. C., Nishida, C. R. and Ortiz de Montellano, P. R (1997) Characterization of human liver inducible nitric oxide synthase expressed in Escherichia coli. *J. Biol. Chem* **343**, 249-253.

Groves, J. and Wang, C. (2000) Nitric oxide synthase: models and mechanisms. *Curr Opin Chem Biol* **4**, 687-695.

Ghosh, D. K., Wu, C., Pitters, E., Moloney, M., Werner, E. R., Mayer, B., Stuehr, D. J. (1997) Characterization of the inducible nitric oxide synthase oxygenase domain identifies a 49 amino acid segment required for subunit dimerization and tetrahydrobiopterin interaction. *Biochem* **36**, 10609-10619.

Ji, H., Li, H., flinspach, M., Poulos, T. L. and Silverman, R. B. (2003) Computer modeling of selective regions in the active site of nitric oxide synthases: implication for the design of isoform-selective inhibitors. *J Med Chem* **46**, 5700-5711.

Ji, H., Li, H., Martasek, P., Roman, L. J.,Poulos, T. L. and Silverman, R. B. (2009) Discovery of highly potent and selective inhibitors of neuronal nitric oxide synthase by fragment hopping. *J Med Chem* **52**, 779-797.

Hobbs, A. J., Higgs, A. and Moncada, S. (1999) Inhibitotion of nitric oxide synthase as a potential therapeutic target. *Biomedical* **39**, 191-220.

Huang, H., Martásek, P., Roman, L. J., and Silverman, R. B. (2000) Synthesis and evaluation of Peptidomimetics as selective inhibitors and active site probes of nitric oxide synthases. *Med Chem* **43**, 2938-2945.

Igarashi, J., Li, H., Jamal, J., ji, H., Fang, J., Lawton, G. R., Silverman, R. B. and Poulos, T. L. (2009) Crystal structures of constitutive nitric oxide synthases in complex with de novo designed inhibitors. *J Med Chem* **52**, 2060-2066.

Kroncke, K., Fehsel, K., Kolb-Bachofen, V. (1998) Inducible nitric oxide synthase in human diseases. *Clin Exp Immunol* **113**, 147-156.

Knowles, R. G. and Moncada, S. (1994) Nitric oxide synthases in mammals. *Biochem* **298**, 249-258.

Leavitt, S and Freire, E (2001) Direct measurement of protein binding energetics by isothermal titration calorimetry. *Biol and Biochem* **5**, 560-566.

Li, H., Raman, C., Martásek, P., Masters, B. and Poulos, T. (2001) Crystallographic studies on endothelial nitric oxide synthase complexed with nitric oxide and mechanism-based inhibitors. *Biochem* **40**, 5399-5406.

Maddaford, T., Dibrov, E., Hurtado, C. and Pierce, G. (2009) Reduced expression of the Na^{+}/Ca^{2+} exchanger in adult cardiomyocytes via adenovirally delivered shRNA results in resistance to simulated ischemic injury. *Am J Physiol Heart Circ Physiol* **298**, 360-366.

Matter H, Kumar, H., Fedorov, R., Frey, A., Kotsonis, P., Hartmann, E., Fröhlich, L., Reif, A., Pfleiderer, W., Scheurer, P., Ghosh, D., Schlichting, I. and Schmidt, H. (2005) Structural analysis of isoform-specific inhibitors targeting the tetrahydrobiopterin binding site of human nitric oxide synthases. *J Med Chem* **48**, 4783-4792.

Newton, D. C. (1997) A comparative study of the reductase domain from the inducible and neuronal forms of nitric oxide synthase and their interactions with camodulin. MSc thesis in Chemistry, University of Waterloo, Waterloo.

Raman, C. S., Li, H., Martasek, P., Kral, V., Masters, B. S. and Poulos, T. l. (1998) Crystal structure of constitutive endothelial nitric oxide synthase: a paradigm for pterin function involving a novel metal center. *Cell* **95**, 939-950.

Rafferty, S. P., Boyington, J. C., Kulansky, R., Sun, P. and Malech, H. L (1999) Stoichiometric arginine binding in the oxygenase domain of inducible nitric oxide synthase requires a single molecule of tetrahydrobiopterin per dimer. *Biochem Biophys Res Commun* **257**, 344-347.

Sabat, J., Stuehr, D. J., Yeh, S. R., Rousseau, D. L. (2009) Characterization of the proximal ligand in the P420 form of inducible nitric oxide synthase. *J Am Chem Soc* **131**, 12186-12192.

Saleron, L., Sorrenti, V., Giacomo, C. D., Romo, G. and Siracusa, M. A. (2002) Progress in the development of selective nitric oxide synthase (NOS) inhibitors. *Curr Pharm Des* **8**, 177-200.

Silverman, R.B. (2009) Design of selective neuronal nitric oxide synthase inhibitors for the prevention and treatment of neurodegenerative diseases. *Acc Chem Res* **42**, 439-451.

Spratt, D. E. (2008) Calmodulin binding and activation of mammalian nitric oxide synthase. PhD thesis in Chemistry, University of Waterloo, Waterloo.

Stuehr, D. J. (1999) Mammalian nitric oxide synthases. *Immunology* **1411,** 217-230.

Suh, N., Honda, T., Finlay, H., Barchowsky, A., Williams, C., Benoit, N., Xie, Q., Nathan, C., Gribble, G. and Sporn, M. (1998) Novel triterpenoids suppress inducible nitric oxide synthase (iNOS) and inducible cyclooxygenase (COX-2) in mouse macrophages. *Cancer Res **58**,* 717-723.

Tiong, K. H., Yiap, B. C., Tan, E. L., Iamail. R. and Ong, C. E. (2010) Molecular cloning and functional analysis of human cytochrome P450 2A6 (CYP2A6). *Mol Biol Biotechnol* **18**, 351-357.

Van den ent, F. and Lowe, J. (2006) RF cloning: A restriction –free method for inserting target genes into plasmids. *Biochem Biophys* **67**, 67-74.

Vallance, P. and Collier, J. (1994) Fortnightly review biology and clinical relevance of nitric oxide. *Clin Pharmaco* **309**,453-457.

Weber, P. C. and Salemme, F. R. (2003) Applications of calorimetric methods to drug discovery and the study of protein interactions. *Curr Opin Struct Biol* **13**, 115-121.

Zakariassen, H., Cederkvist, F. H. and Harbitz, E. (2008) Thermodynamic analysis of L-Arginine and $N^{(\omega)}$-Hydroxy-l-Arginine binding to nitric oxide synthase. *Biochim Biophys Acta, Proteins Proteomics* **1784**, 806-810.